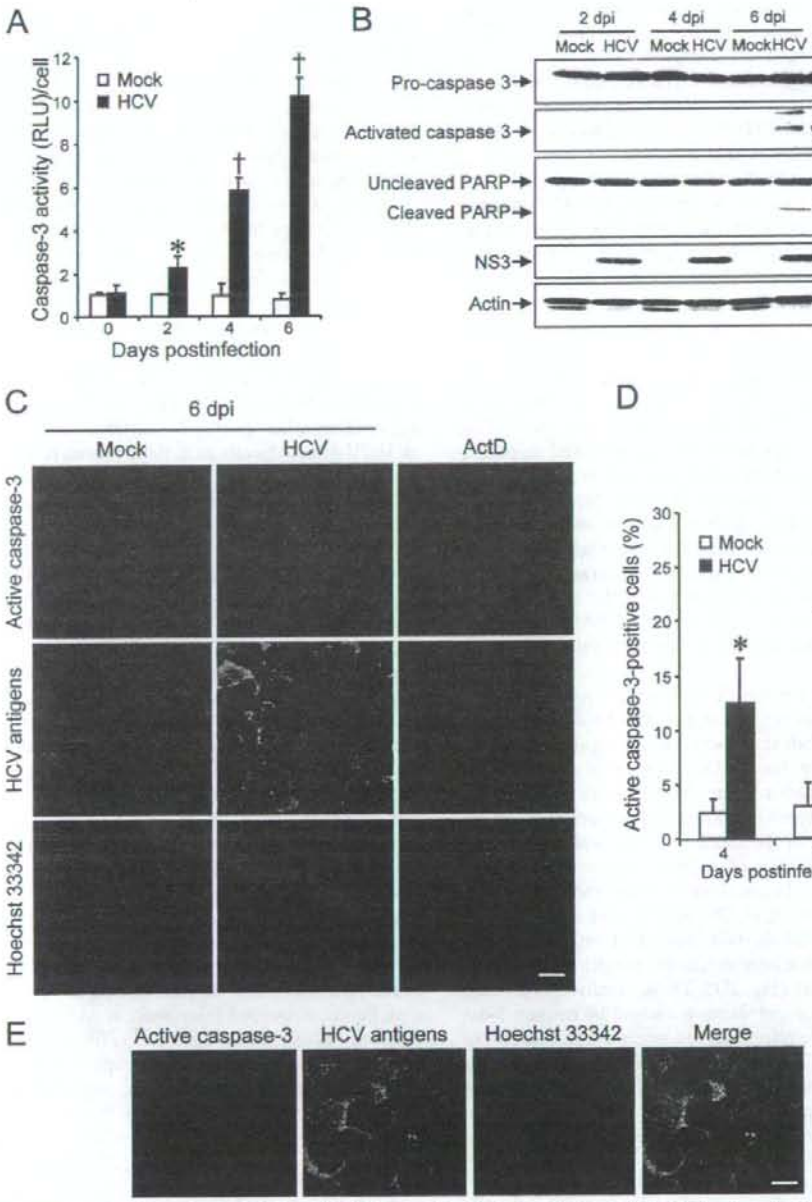

FIG. 2. HCV infection activates caspase 3 in Huh7.5 cells. (A) Caspase 3 activities in cells infected with HCV and mock-infected controls. The caspase 3 activity of the control cells at day 0 postinfection was arbitrarily expressed as 1.0. *, $P < 0.05$; †, $P < 0.01$ (compared with the control). Data represent means ± standard deviations (SD) of three independent experiments. (B) Immunoblot analysis to detect the activated form of caspase 3 (~17 kDa) and cleavage product of PARP (~85 kDa) in HCV-infected cells and the mock-infected control at 2, 4, and 6 days postinfection (dpi). Huh7.5 cells treated with actinomycin D (ActD; 50 ng/ml) for 30 h served as a positive control. Amounts of actin were measured as an internal control to verify an equal amount of sample loading. (C) Huh7.5 cells infected with HCV or mock infected were subjected to indirect immunofluorescence analysis at 6 dpi. Cells treated with ActD (50 ng/ml) for 30 h served as a positive control. After fixation and permeabilization, the cells were incubated with anti-active caspase 3 rabbit polyclonal antibody followed by Cy3-labeled donkey anti-rabbit IgG (top) and with an HCV-infected patient's serum followed by FITC-labeled goat anti-human IgG (middle). The cells were then stained with Hoechst 33342 for the nuclei (bottom). Scale bar, 20 μm. (D) Quantification of active caspase 3-expressing cells. The percentages of cells expressing active caspase 3 were determined for HCV-infected cultures and mock-infected controls. Data represent means ± SD of three independent experiments. *, $P < 0.05$, compared with the control. (E) Nuclear translocation of active caspase 3 in HCV-infected cells. Subcellular localization of active caspase 3 in HCV-infected cells was examined by indirect immunofluorescence analysis at 6 days postinfection as described in the legend for panel C. Scale bar, 5 μm.

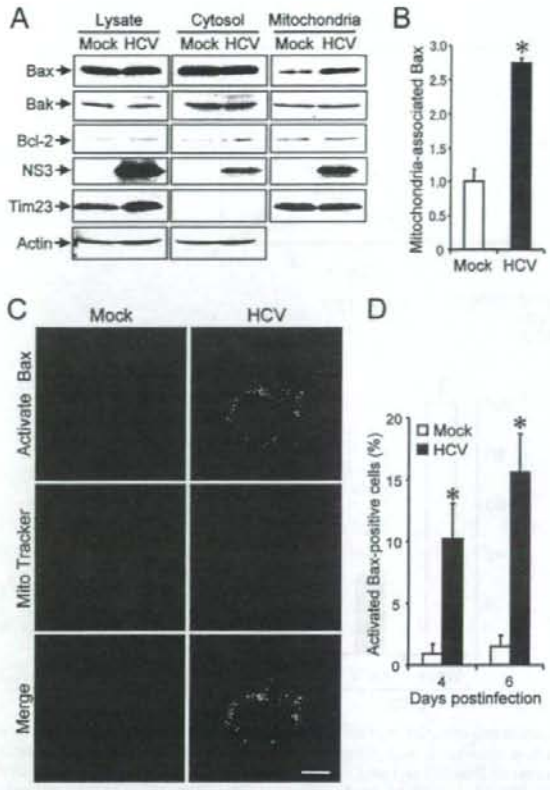

FIG. 3. HCV infection induces Bax activation in Huh7.5 cells. (A) Accumulation of Bax on the mitochondria in HCV-infected Huh7.5 cells. Cytosolic and mitochondrial fractions as well as whole-cell lysates were prepared from HCV-infected cells and the mock-infected control at 6 days postinfection and analyzed by immunoblotting using antibodies against Bax, Bak, Bcl-2, NS3, Tim23, and actin. Amounts of Tim23, a mitochondrion-specific protein, were measured to verify equal amounts of mitochondrial fractions. Amounts of actin were measured to verify equal amounts of whole-cell lysates and cytosolic fractions. (B) The intensities of the bands of mitochondrion-associated Bax in HCV-infected cells and the mock-infected control were quantified. The intensity of the mock-infected control was arbitrarily expressed as 1.0. Data represent means ± standard deviations (SD) of three independent experiments. *, $P < 0.01$, compared with the control. (C) Conformational change of Bax in HCV-infected cells. Huh7.5 cells infected with HCV and the mock-infected control were subjected to indirect immunofluorescence analysis at 6 days postinfection. After incubation with MitoTracker (middle row), the cells were incubated with an antibody specific for the N terminus of Bax (NT antibody), followed by Alexa Fluor 488-labeled goat anti-rabbit IgG (top row). Merged images are shown on the bottom. Scale bar, 10 μm. (D) Quantification of activated Bax-positive cells. The percentages of cells expressing activated Bax were determined for HCV-infected cultures and the mock-infected control. Data represent means ± SD of three independent experiments. *, $P < 0.01$, compared with the control.

HCV antigens. This observation implies the possibility that an indirect effect(s) of HCV infection, in addition to a direct effect of an HCV protein, as observed for NS3/4A (43), is involved in mitochondrial swelling and/or aggregation.

Electron microscopic analysis also demonstrated swelling and structural alterations of mitochondria in HCV-infected cells, whereas mitochondria remained intact in the mock-infected control (Fig. 5C). This result suggests a detrimental effect of HCV infection on the volume homeostasis and morphology of mitochondria and is consistent with previous observations that liver tissues from HCV-infected patients showed morphological changes in mitochondria (3).

Mitochondrial swelling and the morphological change of mitochondrial cristae are associated with cytochrome *c* release (27, 54). We then examined the effect of HCV infection on cytochrome *c* release in Huh7.5 cells. The result clearly demonstrated cytochrome *c* release from the mitochondria to the cytoplasm in HCV-infected cells but not in the mock-infected control (Fig. 6A). The release of cytochrome *c* from mitochondria is known to induce activation of caspase 9 (31). We then analyzed caspase 9 activities in the cells. As shown in Fig. 6B, caspase 9 activities in HCV-infected cells increased to levels that were ca. five times higher than that in the control cells at 4 and 6 days postinfection.

HCV infection induces a marginal degree of caspase 8 activation. In addition to the mitochondrial death (intrinsic) pathway described above, the extrinsic cell death pathway, which is initiated by the TNF family members and mediated by activated caspase 8 (31, 62), is also the focus of attention in the study of apoptosis. Therefore, we examined caspase 8 activities in HCV-infected cells and the mock-infected control. As shown in Fig. 6C, caspase 8 activities in HCV-infected cells increased to a level that was ca. two times higher than that in the control cells at 4 and 6 days postinfection. This increase was much smaller than that observed for caspase 9 activation (Fig. 6B).

HCV infection induces increased production of mitochondrial reactive oxygen species (ROS). The production of ROS, such as superoxide, by mitochondria is the major cause of cellular oxidative stress (8), and a possible link between ROS production and Bax activation has been reported (18, 42). Therefore, we next examined the mitochondrial ROS production in HCV- and mock-infected cells by using MitoSOX, a fluorescent probe specific for superoxide that selectively accumulates in the mitochondrial compartment. As shown in Fig. 7A and B, approximately 25% of HCV-infected cells displayed a much higher signal than did the mock-infected control. This result suggests that oxidative stress is induced by HCV infection.

HCV infection does not induce ER stress. It is well known that HCV nonstructural proteins form the replication complex on the endoplasmic reticulum (ER) membrane (4, 19, 39, 46). It was recently reported that HCV infection (55) as well as the transfection of the full-length HCV replicon (17) and the expression of the entire HCV polyprotein (14) induced an ER stress response. Therefore, we tested whether HCV infection in our system induces ER stress. We adopted increased expression of GRP78 and GRP94 as indicators of ER stress (34) and, as a positive control, used tunicamycin to induce ER stress (20, 25). As had been expected, the expression levels of GRP78 and GRP94 were markedly increased in Huh7.5 cells when cells were treated with tunicamycin for 48 h (Fig. 8, right). On the other hand, HCV infection did not alter expression levels of GRP78 or GRP94 at 2, 4, or 6 days postinfection compared

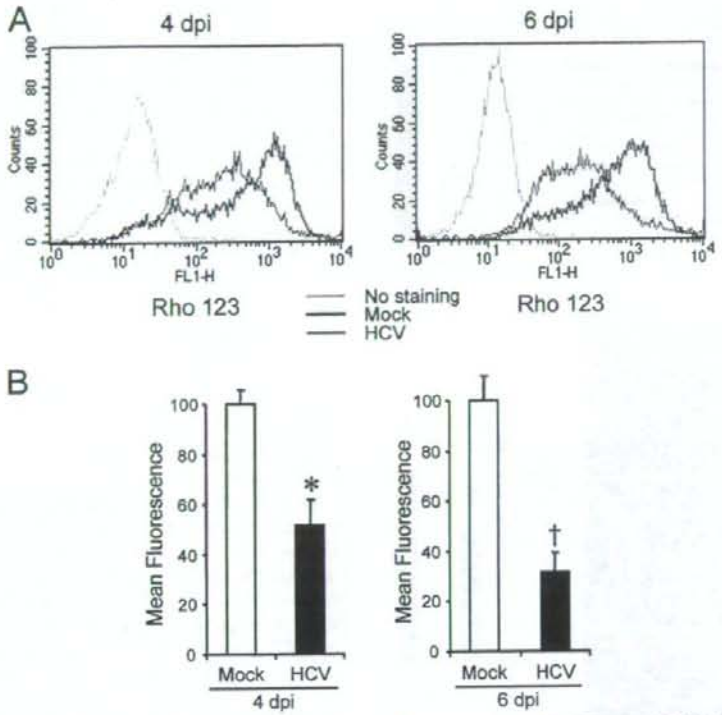

FIG. 4. HCV infection induces disruption of the mitochondrial transmembrane potential in Huh7.5 cells. (A) Huh7.5 cells infected with HCV and the mock-infected control were stained with Rho123 and subjected to flow cytometric analysis to measure the mitochondrial transmembrane potential at 4 and 6 days postinfection (dpi). The red and black lines represent Rho123 staining of HCV-infected cells and the mock-infected control, respectively. The green profiles represent staining of the cells with PBS alone. (B) Mean fluorescence intensities of HCV-infected cells and the mock-infected control at 4 and 6 dpi. Data represent means ± standard deviations (SD) of three independent experiments. *, $P < 0.05$; †, $P < 0.01$ (compared with the control).

with those for the mock-infected control (Fig. 8). This result suggests that ER stress, if there is any, is marginal and does not play an important role in HCV-induced apoptosis in Huh7.5 cells.

DISCUSSION

The mitochondrion is an important organelle for cell survival and death and plays a crucial role in regulating apoptosis. An increasing body of evidence suggests that apoptosis occurs in the livers of HCV-infected patients (1, 2, 9) and that HCV-associated apoptosis involves, at least partly, a mitochondrion-mediated pathway (2). In those clinical settings, however, it is not clear whether apoptosis is mediated by host immune responses through the activity of cytotoxic T lymphocytes or whether it is mediated directly by HCV replication and/or protein expression itself. In experimental settings, ectopic expression of HCV core (13, 36), E2 (12), and NS4A (43) has been shown to induce mitochondrion-mediated apoptosis in cultured cells. However, these observations need to be verified in the context of virus replication. The recent development of an efficient HCV infection system in cell culture (37, 66, 71) has allowed us to investigate whether HCV replication directly causes apoptosis. In the present study, we have demonstrated that HCV infection induces Bax-triggered, mitochondrion-mediated, caspase 3-dependent apoptosis, as evidenced by increased accumulation of Bax on mitochondria and its conformational change (Fig. 3), decreased mitochondrial transmembrane potential (Fig. 4), and mitochondrial swelling (Fig. 5), which lead to the release of cytochrome *c* from the mitochondria (Fig. 6A) and subsequent activation of caspase 9 and caspase 3 (Fig. 6B and 2, respectively).

We also observed increased production of mitochondrial superoxide in HCV-infected cells (Fig. 7). This result is consistent with previous observations that expression of the entire HCV polyprotein (47) or HCV replication (60) enhanced production of ROS, including superoxide, through deregulation of mitochondrial calcium homeostasis. ROS, which are produced through the mitochondrial respiratory chain (8), were reported to trigger conformational change, dimerization, and mitochondrial translocation of Bax (18, 42). It is likely, therefore, that activation of Bax in HCV-infected cells is mediated, at least partly, through increased production of ROS in the mitochondria. Kim et al. (29) reported that ROS is a potent activator of c-Jun N-terminal protein kinase, which can phosphorylate Bax, leading to its activation and mitochondrial translocation. In

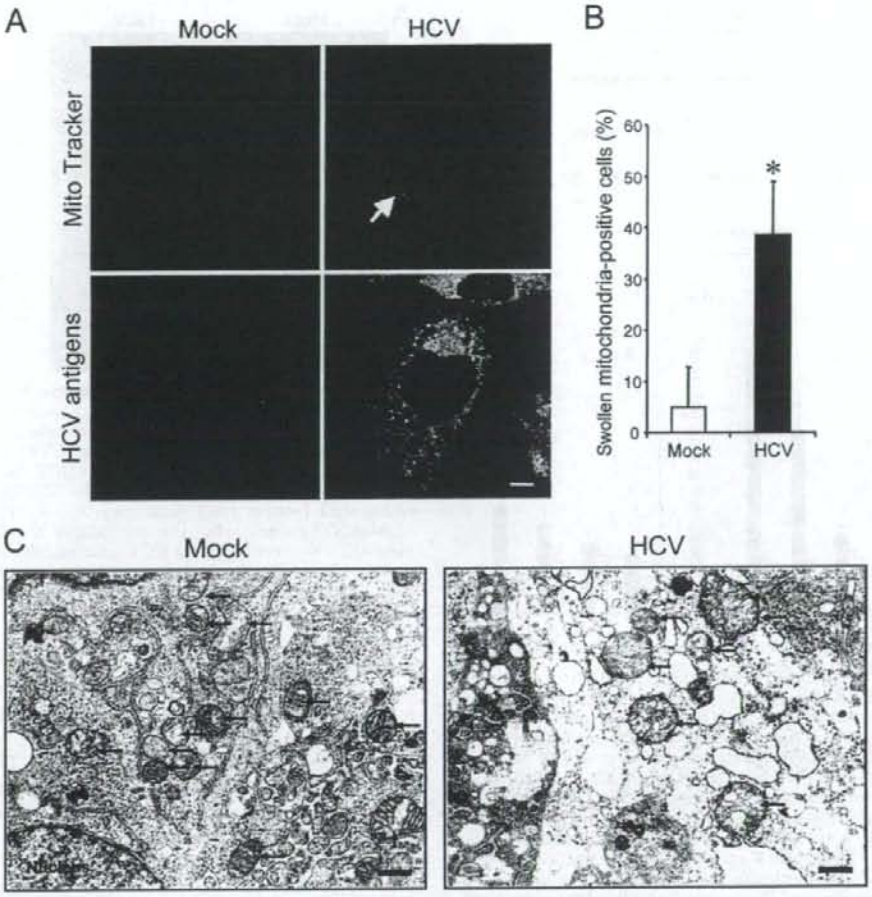

FIG. 5. HCV infection induces mitochondrial morphology changes in Huh7.5 cells. (A) Fluorescence microscopy analysis. Mitochondrial morphologies of HCV-infected cells and the mock-infected control at 6 days postinfection were examined by confocal microscopy. The cells were directly incubated with MitoTracker (upper row) and then stained for HCV antigens by using an HCV-infected patient's serum, followed by FITC-labeled goat anti-human IgG (bottom row). Scale bar, 5 μm. (B) Quantification of swollen mitochondrion-positive cells. The percentages of cells exhibiting swollen and/or aggregated mitochondria were determined for HCV-infected cultures and the mock-infected control. Data represent means ± standard deviations of three independent experiments. *, $P < 0.01$, compared with the control. (C) Electron microscopic analysis. Mitochondrial morphologies of HCV-infected cells and the mock-infected control at 6 days postinfection were examined by electron microscopy. Arrows indicate mitochondria. Scale bar, 1 μm.

this connection, HCV core protein has been shown to play a role in generating mitochondrial ROS (30). It was also reported that HCV core protein bound to the 14-3-3ε protein to dissociate Bax from the Bax/14-3-3ε complex, thereby promoting the Bax translocation to the mitochondria (36).

In addition to the caspase 9 activation that is mediated through the mitochondrial death (intrinsic) pathway, caspase 8 activation was seen in HCV-infected cells, though to a lesser extent (Fig. 6B and C). Caspase 8 is a key component of the extrinsic death pathway initiated by the TNF family members (31, 62). This pathway involves death receptors, such as Fas, TNF receptor, and TNF-related apoptosis-inducing ligand (TRAIL) receptors, which transduce signals to induce apoptosis upon binding to their respective ligands (52). In HCV-infected patients, the Fas-mediated signal pathway is involved in apoptosis of virus-infected hepatocytes (24). It was also reported that HCV (JFH1 strain) infection induced apoptosis through a TRAIL-mediated pathway in LH86 cells (72). On the other hand, a caspase 9-mediated activation of caspase 8, which is considered a cross talk between the intrinsic and the extrinsic death pathways, in certain cell systems was also reported (10, 11, 65). Whether the observed caspase 8 activation in HCV-infected cells was mediated through the extrinsic death pathway initiated by a cytokine(s) produced in the culture or whether it was mediated through the cross talk between the intrinsic and the extrinsic death pathways awaits further investigation. In this connection, activated caspase 8 is known to cleave the proapoptotic protein Bid to generate the Bid

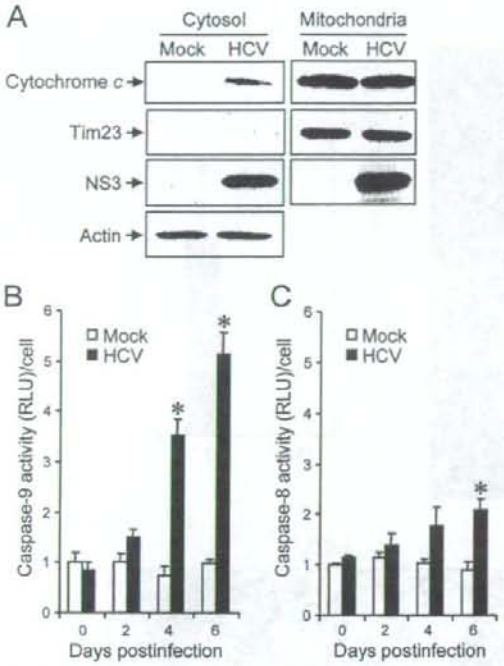

FIG. 6. HCV infection induces cytochrome *c* release and caspase 9 activation in Huh7.5 cells. (A) Cytochrome *c* release. Mitochondrial and cytosolic fractions were prepared from HCV-infected cells and the mock-infected control at 6 days postinfection and analyzed by immunoblotting using antibodies against cytochrome *c*, Tim23, NS3, and actin. Can Get Signal (Toyobo, Osaka, Japan) was used to obtain stronger signals for cytochrome *c*. Amounts of Tim23 and actin were measured to verify equal amounts of mitochondrial and cytosolic fractions, respectively. Also, Tim23 was used to show successful separation of mitochondria. (B) Caspase 9 activation. Caspase 9 activities in cells infected with HCV and mock-infected controls were measured at 0, 2, 4, and 6 days postinfection. The caspase 9 activity of the control cells at day 0 postinfection was arbitrarily expressed as 1.0. Data represent means ± standard deviations (SD) of three independent experiments. *, $P < 0.05$, compared with the control. (C) HCV infection induces a marginal degree of caspase 8 activation. Caspase 8 activities in cells infected with HCV and mock-infected controls were measured at 0, 2, 4, and 6 days postinfection. The caspase 8 activity of the control cells at day 0 postinfection was arbitrarily expressed as 1.0. Data represent means ± SD of three independent experiments. *, $P < 0.05$, compared with the control.

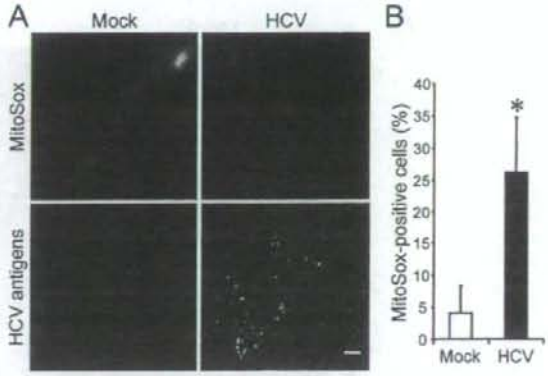

FIG. 7. HCV infection induces increased production of mitochondrial superoxide in Huh7.5 cells. (A) Mitochondrial superoxide production in HCV-infected cells and the mock-infected control was examined at 6 days postinfection. Cells were directly incubated with MitoSOX (upper row) and then stained for HCV antigens by using an HCV-infected patient's serum, followed by FITC-labeled goat anti-human IgG (bottom row). Scale bar, 10 μm. (B) Quantification of MitoSOX-stained cells. The percentages of cells stained with MitoSOX were determined for HCV-infected cultures and the mock-infected control. Data represent means ± standard deviations of three independent experiments. *, $P < 0.05$, compared with the control.

cleavage product truncated Bid (tBid), which facilitates the activation of Bax (63, 68). Under our experimental conditions, however, tBid was barely detected in HCV-infected cells even at 6 days postinfection (data not shown). It is thus likely that caspase 8 activation is marginal and is not the primary cause of Bax activation in our experimental system.

HCV protein expression and HCV RNA replication take place primarily in the ER or an ER-like membranous structure (39, 46). Like other members of the family *Flaviviridae*, such as dengue virus (69), Japanese encephalitis virus (69), West Nile virus (41), and bovine viral diarrhea virus (26), HCV has been reported to induce ER stress in the host cells (5, 14, 17, 55, 60). ER stress is triggered by perturbations in normal ER function, such as the accumulation of unfolded or misfolded proteins in the lumen. On the other hand, in response to ER stress, the unfolded protein response (UPR) is activated to alleviate the ER stress by stimulating protein folding and degradation in the ER as well as by inhibiting protein synthesis (7). The UPR of the host cell is disadvantageous for progeny virus production and may therefore be considered an antiviral host cell response. It was reported that, to counteract the disadvantageous UPR so as to maintain viral protein synthesis, HCV RNA replication suppressed the IRE1-XBP1 pathway, which is responsible for protein degradation upon UPR (59). Also, HCV E2 was shown to inhibit the double-stranded RNA-activated protein kinase-like ER-resident kinase (PERK), which attenuates protein synthesis during ER stress by phosphorylating the alpha subunit of eukaryotic translation initiation factor 2 (45). It is reasonable, therefore, to assume that HCV-infected cells may not necessarily exhibit typical responses to ER stress. In fact, our results revealed that HCV infection in Huh7.5 cells did not enhance

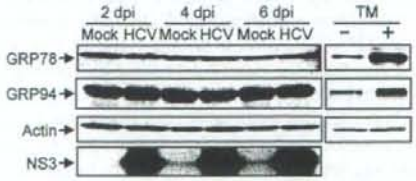

FIG. 8. HCV infection does not induce ER stress in Huh7.5 cells. Huh7.5 cells infected with HCV and mock-infected controls were harvested at 2, 4, and 6 days postinfection (dpi), and the whole-cell lysates were subjected to immunoblot analysis using antibodies against GRP78, GRP94, NS3, and actin. Amounts of actin were measured to verify equal amounts of sample loading. Huh7.5 cells treated with tunicamycin (TM; 5 μg/ml) for 48 h served as a positive control.

expression of GRP78 and GRP94, which are ER stress-induced chaperone proteins (Fig. 8). Our result thus implies the possibility that ER stress is not crucially involved in HCV-induced apoptosis in Huh7.5 cells. Taking advantage of this phenomenon, we could demonstrate that an ER stress-independent, mitochondrion-mediated pathway plays an important role in HCV-induced apoptosis. In this connection, Korenaga et al. (30) reported that HCV core protein increased ROS production in isolated mitochondria, independently of ER stress, by selectively inhibiting electron transport complex I activity.

In this study, we observed that increased ROS production, Bax activation, and caspase 3 activation were detectable in approximately 15% to 25% of HCV antigen-positive Huh7.5cells at 6 days postinfection (Fig. 7B, 3D, and 2D, respectively). On the other hand, >90% of the cells in the cultures were confirmed positive for HCV antigens (Fig. 1B). These results imply the possibility that HCV establishes persistent infection in Huh7.5 cells, with a minor fraction of virus-infected cells beginning to undergo apoptosis after a prolonged period of time. Alternatively, it is possible that Huh7.5 cells, though being derived from a cell line (6), are a mixture of two sublineages, with one sublineage being apoptosis prone and the other apoptosis resistant. To test the latter possibility, further cloning of Huh7.5 cells is now under way in our laboratory.

In conclusion, our present results collectively suggest that HCV infection induces apoptosis through a Bax-triggered, mitochondrion-mediated, caspase 3-dependent pathway.

ACKNOWLEDGMENTS

We are grateful to C. M. Rice (Center for the Study of Hepatitis C, The Rockefeller University) for providing pFL-J6/JFH1 and Huh7.5 cells.

This work was supported in part by grants-in-aid for scientific research from the Ministry of Education, Culture, Sports, Science and Technology (MEXT) and the Ministry of Health, Labor and Welfare, Japan.

This study was carried out as part of the Program of Founding Research Centers for Emerging and Reemerging Infectious Diseases, MEXT, Japan. This study was also part of the 21st Century Center of Excellence Program at Kobe University Graduate School of Medicine.

REFERENCES

1. **Bantel, H., A. Lügering, C. Poremba, N. Lügering, J. Heid, W. Domschke, and K. Schulze-Osthoff.** 2001. Caspase activation correlates with the degree of inflammatory liver injury in chronic hepatitis C virus infection. Hepatology **34:**758–767.
2. **Bantel, H., and K. Schulze-Osthoff.** 2003. Apoptosis in hepatitis C virus infection. Cell Death Differ. **10:**S48–S58.
3. **Barbaro, G., G. Di Lorenzo, A. Asti, M. Ribersani, G. Belloni, B. Grisorio, G. Filice, and G. Barbarini.** 1999. Hepatocellular mitochondrial alterations in patients with chronic hepatitis C: ultrastructural and biochemical findings. Am. J. Gastroenterol. **94:**2198–2205.
4. **Bartenschlager, R., M. Frese, and T. Pietschmann.** 2004. Novel insights into hepatitis C virus replication and persistence. Adv. Virus Res. **63:**171–180.
5. **Benali-Furet, N. L., M. Chami, L. Houel, F. De Giorgi, F. Vernejoul, D. Lagorce, L. Buscail, R. Bartenschlager, F. Ichas, R. Rizzuto, and P. Paterlini-Bréchot.** 2005. Hepatitis C virus core triggers apoptosis in liver cells by inducing ER stress and ER calcium depletion. Oncogene **24:**4921–4933.
6. **Blight, K. J., J. A. McKeating, and C. M. Rice.** 2002. Highly permissive cell lines for subgenomic and genomic hepatitis C virus RNA replication. J. Virol. **76:**13001–13014.
7. **Boyce, M., and J. Yuan.** 2006. Cellular response to endoplasmic reticulum stress: a matter of life or death. Cell Death Differ. **13:**363–373.
8. **Brookes, P. S.** 2005. Mitochondrial H^+ leak and ROS generation: an odd couple. Free Radic. Biol. Med. **38:**12–23.
9. **Calabrese, F., P. Pontisso, E. Pettenazzo, L. Benvegnù, A. Vario, L. Chemello, A. Alberti, and M. Valente.** 2000. Liver cell apoptosis in chronic hepatitis C correlates with histological but not biochemical activity or serum HCV-RNA levels. Hepatology **31:**1153–1159.
10. **Camacho-Leal, P., and C. P. Stanners.** 2008. The human carcinoembryonic antigen (CEA) GPI anchor mediates anoikis inhibition by inactivation of the intrinsic death pathway. Oncogene **27:**1545–1553.
11. **Chae, Y. J., H. S. Kim, H. Rhim, B. E. Kim, S. W. Jeong, and I. K. Kim.** 2001. Activation of caspase-8 in 3-deazaadenosine-induced apoptosis of U-937 cells occurs downstream of caspase-3 and caspase-9 without Fas receptor-ligand interaction. Exp. Mol. Med. **4:**284–292.
12. **Chiou, H. L., Y. S. Hsieh, M. R. Hsieh, and T. Y. Chen.** 2006. HCV E2 may induce apoptosis of Huh-7 cells via a mitochondrial-related caspase pathway. Biochem. Biophys. Res. Commun. **345:**453–458.
13. **Chou, A. H., H. F. Tsai, Y. Y. Wu, C. Y. Hu, L. H. Hwang, P. I. Hsu, and P. N. Hsu.** 2005. Hepatitis C virus core protein modulates TRAIL-mediated apoptosis by enhancing Bid cleavage and activation of mitochondria apoptosis signaling pathway. J. Immunol. **174:**2160–2166.
14. **Christen, V., S. Treves, F. H. Duong, and M. H. Heim.** 2007. Activation of endoplasmic reticulum stress response by hepatitis viruses up-regulates protein phosphatase 2A. Hepatology **46:**558–565.
15. **Ciccaglione, A. R., C. Marcantonio, A. Costantino, M. Equestre, and M. Rapicetta.** 2003. Expression of HCV E1 protein in baculovirus-infected cells: effects on cell viability and apoptosis induction. Intervirology **46:**121–126.
16. **Ciccaglione, A. R., C. Marcantonio, E. Tritarelli, M. Equestre, F. Magurano, A. Costantino, L. Nicoletti, and M. Rapicetta.** 2004. The transmembrane domain of hepatitis C virus E1 glycoprotein induces cell death. Virus Res. **104:**1–9.
17. **Ciccaglione, A. R., C. Marcantonio, E. Tritarelli, M. Equestre, F. Vendittelli, A. Costantino, A. Geraci, and M. Rapicetta.** 2007. Activation of the ER stress gene gadd153 by hepatitis C virus sensitizes cells to oxidant injury. Virus Res. **126:**128–138.
18. **D'Alessio, M., M. De Nicola, S. Coppola, G. Gualandi, L. Pugliese, C. Cerella, S. Cristofanon, P. Civitareale, M. R. Ciriolo, A. Bergamaschi, A. Magrini, and L. Ghibelli.** 2005. Oxidative Bax dimerization promotes its translocation to mitochondria independently of apoptosis. FASEB J. **19:**1504–1506.
19. **Egger, D., B. Wölk, R. Gosert, L. Bianchi, H. E. Blum, D. Moradpour, and K. Bienz.** 2002. Expression of hepatitis C virus proteins induces distinct membrane alterations including a candidate viral replication complex. J. Virol. **76:**5974–5984.
20. **Elbein, A. D.** 1987. Inhibitors of the biosynthesis and processing of N-linked oligosaccharide chains. Annu. Rev. Biochem. **56:**497–534.
21. **Erdtmann, L., N. Franck, H. Lerat, J. Le Seyec, D. Gilot, I. Cannie, P. Gripon, U. Hibner, and C. Guguen-Guillouzo.** 2003. The hepatitis C virus NS2 protein is an inhibitor of CIDE-B-induced apoptosis. J. Biol. Chem. **278:**18256–18264.
22. **Griffin, S., D. Clarke, C. McCormick, D. Rowlands, and M. Harris.** 2005. Signal peptide cleavage and internal targeting signals direct the hepatitis C virus p7 protein to distinct intracellular membranes. J. Virol. **79:**15525–15536.
23. **Hidajat, R., M. Nagano-Fujii, L. Deng, M. Tanaka, Y. Takigawa, S. Kitazawa, and H. Hotta.** 2005. Hepatitis C virus NS3 protein interacts with ELKS-8 and ELKS-α, members of a novel protein family involved in intracellular transport and secretory pathways. J. Gen. Virol. **86:**2197–2208.
24. **Jarmay, K., G. Karacsony, Z. Ozsvar, I. Nagy, J. Lonovics, and Z. Schaff.** 2002. Assessment of histological feature in chronic hepatitis C. Hepatogastroenterology **49:**239–243.
25. **Jiang, C. C., L. H. Chen, S. Gillespie, K. A. Kiejda, N. Mhaidat, Y. F. Wang, R. Thorne, X. D. Zhang, and P. Hersey.** 2007. Tunicamycin sensitizes human melanoma cells to tumor necrosis factor-related apoptosis-inducing ligand-induced apoptosis by up-regulation of TRAIL-R2 via the unfolded protein response. Cancer Res. **67:**5880–5888.
26. **Jordan, R., L. Wang, T. M. Graczyk, T. M. Block, and P. R. Romano.** 2002. Replication of a cytopathic strain of bovine viral diarrhea virus activates PERK and induces endoplasmic reticulum stress-mediated apoptosis of MDBK cells. J. Virol. **76:**9588–9599.
27. **Kaasik, A., D. Safiulina, A. Zharkovsky, and V. Veksler.** 2007. Regulation of mitochondrial matrix volume. Am. J. Physiol. Cell Physiol. **292:**C157–C163.
28. **Kamada, S., U. Kikkawa, Y. Tsujimoto, and T. Hunter.** 2005. Nuclear translocation of caspase-3 is dependent on its proteolytic activation and recognition of a substrate-like protein(s). J. Biol. Chem. **280:**857–860.
29. **Kim, B. J., S. W. Ryu, and B. J. Song.** 2006. JNK- and p38 kinase-mediated phosphorylation of Bax leads to its activation and mitochondrial translocation and to apoptosis of human hepatoma HepG2 cells. J. Biol. Chem. **281:**21256–21265.
30. **Korenaga, M., T. Wang, Y. Li, L. A. Showalter, T. Chan, J. Sun, and S. A. Weinman.** 2005. Hepatitis C virus core protein inhibits mitochondrial electron transport and increases reactive oxygen species (ROS) production. J. Biol. Chem. **280:**37481–37488.
31. **Kumar, S.** 2007. Caspase function in programmed cell death. Cell Death Differ. **14:**32–43.
32. **Lalier, L., P. F. Cartron, P. Juin, S. Nedelkina, S. Manon, B. Bechinger, and**

F. M. Vallette. 2007. Bax activation and mitochondrial insertion during apoptosis. Apoptosis **12**:887–896.
33. **Lan, K. H., M. L. Sheu, S. J. Hwang, S. H. Yen, S. Y. Chen, J. C. Wu, Y. J. Wang, N. Kato, M. Omata, F. Y. Chang, and S. D. Lee.** 2002. HCV NS5A interacts with p53 and inhibits p53-mediated apoptosis. Oncogene **21**:4801–4811.
34. **Lee, A. S.** 2001. The glucose-regulated proteins: stress induction and clinical applications. Trends Biochem. Sci. **26**:504–510.
35. **Lee, S. H., Y. K. Kim, C. S. Kim, S. K. Seol, J. Kim, S. Cho, Y. L. Song, R. Bartenschlager, and S. K. Jang.** 2005. E2 of hepatitis C virus inhibits apoptosis. J. Immunol. **175**:8226–8235.
36. **Lee, S. K., S. O. Park, C. O. Joe, and Y. S. Kim.** 2007. Interaction of HCV core protein with 14-3-3ε protein releases Bax to activate apoptosis. Biochem. Biophys. Res. Commun. **352**:756–762.
37. **Lindenbach, B. D., M. J. Evans, A. J. Syder, B. Wölk, T. L. Tellinghuisen, C. C. Liu, T. Maruyama, R. O. Hynes, D. R. Burton, J. A. McKeating, and C. M. Rice.** 2005. Complete replication of hepatitis C virus in cell culture. Science **309**:623–626.
38. **Lindenbach, B. D., P. Meuleman, A. Ploss, T. Vanwolleghem, A. J. Syder, J. A. McKeating, R. E. Lanford, S. M. Feinstone, M. E. Major, G. Leroux-Roels, and C. M. Rice.** 2006. Cell culture-grown hepatitis C virus is infectious in vivo and can be recultured in vitro. Proc. Natl. Acad. Sci. USA **103**:3805–3809.
39. **Lindenbach, B. D., and C. M. Rice.** 2005. Unravelling hepatitis C virus replication from genome to function. Nature **436**:933–938.
40. **Marusawa, H., M. Hijikata, T. Chiba, and K. Shimotohno.** 1999. Hepatitis C virus core protein inhibits Fas- and tumor necrosis factor alpha-mediated apoptosis via NF-κB activation. J. Virol. **73**:4713–4720.
41. **Medigeshi, G. R., A. M. Lancaster, A. J. Hirsch, T. Briese, W. I. Lipkin, V. Defilippis, K. Früh, P. W. Mason, J. Nikolich-Zugich, and J. A. Nelson.** 2007. West Nile virus infection activates the unfolded protein response, leading to CHOP induction and apoptosis. J. Virol. **81**:10849–10860.
42. **Nie, C., C. Tian, L. Zhao, P. X. Petit, M. Mehrpour, and Q. Chen.** 2008. Cysteine 62 of Bax is critical for its conformational activation and its pro-apoptotic activity in response to H_2O_2-induced apoptosis. J. Biol. Chem. **283**:15359–15369.
43. **Nomura-Takigawa, Y., M. Nagano-Fujii, L. Deng, S. Kitazawa, S. Ishido, K. Sada, and H. Hotta.** 2006. Non-structural protein 4A of Hepatitis C virus accumulates on mitochondria and renders the cells prone to undergoing mitochondria-mediated apoptosis. J. Gen. Virol. **87**:1935–1945.
44. **Oliver, F. J., G. de la Rubia, V. Rolli, M. C. Ruiz-Ruiz, G. de Murcia, and J. M. Murcia.** 1998. Importance of poly(ADP-ribose) polymerase and its cleavage in apoptosis. J. Biol. Chem. **273**:33533–33539.
45. **Pavio, N., P. R. Romano, T. M. Graczyk, S. M. Feinstone, and D. R. Taylor.** 2003. Protein synthesis and endoplasmic reticulum stress can be modulated by the hepatitis C virus envelope protein E2 through the eukaryotic initiation factor 2α kinase PERK. J. Virol. **77**:3578–3585.
46. **Pawlotsky, J. M., S. Chevaliez, and J. G. McHutchison.** 2007. The hepatitis C virus life cycle as a target for new antiviral therapies. Gastroenterology. *132*:1979–1998.
47. **Piccoli, C., R. Scrima, G. Quarato, A. D'Aprile, M. Ripoli, L. Lecce, D. Boffoli, D. Moradpour, and N. Capitanio.** 2007. Hepatitis C virus protein expression causes calcium-mediated mitochondrial bioenergetic dysfunction and nitro-oxidative stress. Hepatology **46**:58–65.
48. **Prikhod'ko, E. A., G. G. Prikhod'ko, R. M. Siegel, P. Thompson, M. E. Major, and J. I. Cohen.** 2004. The NS3 protein of hepatitis C virus induces caspase-8-mediated apoptosis independent of its protease or helicase activities. Virology **329**:53–67.
49. **Ray, R. B., K. Meyer, R. Steele, A. Shrivastava, B. B. Aggarwal, and R. Ray.** 1998. Inhibition of tumor necrosis factor (TNF-α)-mediated apoptosis by hepatitis C virus core protein. J. Biol. Chem. **273**:2256–2259.
50. **Safiulina, D., V. Veksler, A. Zharkovsky, and A. Kaasik.** 2006. Loss of mitochondrial membrane potential is associated with increase in mitochondrial volume: physiological role in neurones. J. Cell. Physiol. **206**:347–353.
51. **Saito, K., K. Meyer, R. Warner, A. Basu, R. B. Ray, and R. Ray.** 2006. Hepatitis C virus core protein inhibits tumor necrosis factor alpha-mediated apoptosis by a protective effect involving cellular FLICE inhibitory protein. J. Virol. **80**:4372–4379.
52. **Schulze-Osthoff, K., D. Ferrari, M. Los, S. Wesselborg, and M. E. Peter.** 1998. Apoptosis signaling by death receptors. Eur. J. Biochem. **254**:439–459.
53. **Schwer, B., S. Ren, T. Pietschmann, J. Kartenbeck, K. Kaehlcke, R. Bartenschlager, T. S. Yen, and M. Ott.** 2004. Targeting of hepatitis C virus core protein to mitochondria through a novel C-terminal localization motif. J. Virol. **78**:7958–7968.
54. **Scorrano, L., M. Ashiya, K. Buttle, S. Weiler, S. A. Oakes, C. A. Mannella, and S. J. Korsmeyer.** 2002. A distinct pathway remodels mitochondrial cristae and mobilizes cytochrome c during apoptosis. Dev. Cell **2**:55–67.
55. **Sekine-Osajima, Y., N. Sakamoto, K. Mishima, M. Nakagawa, Y. Itsui, M. Tasaka, Y. Nishimura-Sakurai, C. H. Chen, T. Kanai, K. Tsuchiya, T. Wakita, N. Enomoto, and M. Watanabe.** 2008. Development of plaque assays for hepatitis C virus-JFH1 strain and isolation of mutants with enhanced cytopathogenicity and replication capacity. Virology **371**:71–85.
56. **Shepard, C. W., L. Finelli, and M. J. Alter.** 2005. Global epidemiology of hepatitis C virus infection. Lancet Infect. Dis. **5**:558–567.
57. **Siavoshian, S., J. D. Abraham, C. Thumann, M. P. Kieny, and C. Schuster.** 2005. Hepatitis C virus core, NS3, NS5A, NS5B proteins induce apoptosis in mature dendritic cells. J. Med. Virol. **75**:402–411.
58. **Tanaka, M., M. Nagano-Fujii, L. Deng, S. Ishido, K. Sada, and H. Hotta.** 2006. Single-point mutations of hepatitis C virus that impair p53 interaction and anti-apoptotic activity of NS3. Biochem. Biophys. Res. Commun. **340**:792–799.
59. **Tardif, K. D., K. Mori, R. J. Kaufman, and A. Siddiqui.** 2004. Hepatitis C virus suppresses the IRE1-XBP1 pathway of the unfolded protein response. J. Biol. Chem. **279**:17158–17164.
60. **Tardif, K. D., G. Waris, and A. Siddiqui.** 2005. Hepatitis C virus, ER stress, and oxidative stress. Trends Microbiol. **13**:159–163.
61. **Tewari, M., L. T. Quan, K. O'Rourke, S. Desnoyers, Z. Zeng, D. R. Beidler, G. G. Poirier, G. S. Salvesen, and V. M. Dixit.** 1995. Yama/CPP32 beta, a mammalian homolog of CED-3, is a CrmA-inhibitable protease that cleaves the death substrate poly (ADP-ribose) polymerase. Cell **81**:801–809.
62. **Thorburn, A.** 2004. Death receptor-induced cell killing. Cell. Signal. **16**:139–144.
63. **Tsujimoto, Y.** 2003. Cell death regulation by the Bcl-2 protein family in the mitochondria. J. Cell. Physiol. **195**:158–167.
64. **Upton, J. P., A. J. Valentijn, L. Zhang, and A. P. Gilmore.** 2007. The N-terminal conformation of Bax regulates cell commitment to apoptosis. Cell Death Differ. **14**:932–942.
65. **Viswanath, V., Y. Wu, R. Boonplueang, S. Chen, F. F. Stevenson, F. Yantiri, L. Yang, M. F. Beal, and J. K. Andersen.** 2001. Caspase-9 activation results in downstream caspase-8 activation and bid cleavage in 1-methyl-4-phenyl-1,2,3,6-tetrahydropyridine-induced Parkinson's disease. J. Neurosci. **21**:9519–9528.
66. **Wakita, T., T. Pietschmann, T. Kato, T. Date, M. Miyamoto, Z. Zhao, K. Murthy, A. Habermann, H. G. Kräusslich, M. Mizokami, R. Bartenschlager, and T. J. Liang.** 2005. Production of infectious hepatitis C virus in tissue culture from a cloned viral genome. Nat. Med. **11**:791–796.
67. **Wang, J., W. Tong, X. Zhang, L. Chen, Z. Yi, T. Pan, Y. Hu, L. Xiang, and Z. Yuan.** 2006. Hepatitis C virus non-structural protein NS5A interacts with FKBP38 and inhibits apoptosis in Huh7 hepatoma cells. FEBS Lett. **580**:4392–4400.
68. **Wei, M. C., W. X. Zong, E. H. Cheng, T. Lindsten, V. Panoutsakopoulou, A. J. Ross, K. A. Roth, G. R. MacGregor, C. B. Thompson, and S. J. Korsmeyer.** 2001. Proapoptotic BAX and BAK: a requisite gateway to mitochondrial dysfunction and death. Science **292**:727–730.
69. **Yu, C. Y., Y. W. Hsu, C. L. Liao, and Y. L. Lin.** 2006. Flavivirus infection activates the XBP1 pathway of the unfolded protein response to cope with endoplasmic reticulum stress. J. Virol. **80**:11868–11880.
70. **Zhivotovsky, B., A. Samali, A. Gahm, and S. Orrenius.** 1999. Caspases: their intracellular localization and translocation during apoptosis. Cell Death Differ. **6**:644–651.
71. **Zhong, J., P. Gastaminza, G. Cheng, S. Kapadia, T. Kato, D. R. Burton, S. F. Wieland, S. L. Uprichard, T. Wakita, and F. V. Chisari.** 2005. Robust hepatitis C virus infection in vitro. Proc. Natl. Acad. Sci. USA **102**:9294–9299.
72. **Zhu, H., H. Dong, E. Eksioglu, A. Hemming, M. Cao, J. M. Crawford, D. R. Nelson, and C. Liu.** 2007. Hepatitis C virus triggers apoptosis of a newly developed hepatoma cell line through antiviral defense system. Gastroenterology **133**:1649–1659.
73. **Zhu, N., A. Khoshnan, R. Schneider, M. Matsumoto, G. Dennert, C. Ware, and M. M. C. Lai.** 1998. Hepatitis C virus core protein binds to the cytoplasmic domain of tumor necrosis factor (TNF) receptor 1 and enhances TNF-induced apoptosis. J. Virol. **72**:3691–3697.

<原　著>

1b型高ウイルス量高齢者C型慢性肝炎に対するPEG IFNα-2b/リバビリン治療（併用療法）の検討

金　守良[1)*]　井本　勉[1)]　婦木　秀一[1)]　金　啓二[2)]
谷口　美幸[3)]　長野　基子[4)]　堀田　博[4)]　勝二　郁夫[4)]
寒原　芳浩[5)]　前川　陽子[6)]　工藤　正俊[7)]　林　祥剛[8)]

要旨：1b型高ウイルスC型慢性肝炎の65歳以上（高齢群）23名（平均年齢69.4歳）と65歳未満（非高齢群）52名（平均年齢53.5歳）を対象にIFNα2b/リバビリン併用療法を比較検討した．著効率と中断率は高齢群37.5%（6/16），30.4%（7/23），非高齢群50%（20/40），23.1%（12/52）で有意差はなく，HCVコア抗原減少率，2-5AS応答率も両群間に有意差を認めなかった．高齢群では著効例は非著効例に比して開始時のAFP値が有意に低値であった（P<0.01）．高齢群では著効・非著効を問わず治療前後でAFP値は有意に低下しており（開始時10.1±9.55 ng/ml，終了時5.18±4.52 ng/ml（P<0.05）），治療により発癌抑制がもたらされた可能性が考えられた．よって，高齢群においては，たとえ著効に至らない場合であっても治療の完遂が重要である．

索引用語：1b型高ウイルス量C型慢性肝炎　PEG IFNα-2b/リバビリン併用療法　高齢者　発癌抑制　AFP

緒　言

C型慢性肝炎は肝硬変や肝癌に進展する重篤な疾患である．近年，C型慢性肝炎の高齢化が顕著であり[1)]，それに伴って肝癌発生も高齢化する傾向にあり，肝癌好発年齢は60歳代になっている[2)]．一方，適切なIFN治療によりC型慢性肝炎の治療がなされ著効に持ち込めれば，肝発癌率を低下させることが示されている[3)]．C型肝炎のゲノタイプについていえば，日本においては70%が1b型で，残りの30%が2a，2b型である．1b型のうち，70%が高ウイルス量の患者である[4)]．こうした1b型高ウイルス量の患者に対して，従来のIFN単独療法は10%以下の低い著効率しかもたらさなかった[5)]．

IFN治療の進歩，すなわちPEG IFNα-2b/リバビリン治療（併用療法）は1b型高ウイルス量患者においても50～60%の高い著効率をもたらしている[6)7)]．ただ，1b型高ウイルス量患者に対するこの併用療法においても，インスリン抵抗性[8)9)]，肝脂肪化[10)]，肝線維化の進んだ症例，肥満例，女性，高齢者などで著効率が低い傾向にある[8)]．しかし，1b型高ウイルス量高齢者C型慢性肝炎に対する併用療法に関してその著効率，著効に関する因子，及び発癌抑制の検討は少ない．

この併用療法のもう一つの問題点はPEG IFNα-2b投与による食欲不振，全身倦怠，血球減少の副作用に加えて，リバビリン投与による貧血などの副作用が顕著なこと，とりわけ高齢者においてその副作用のために治療の継続を困難にしていることである[11)～13)]．ただ，その中断時期，中断率，中断理由の検討は少ない．そこで，1b型高ウイルス量高齢者C型慢性肝炎に対する併用療法の現状を把握する目的で65歳以上の高齢者の症例を65歳未満の症例と比較した．

1）神戸朝日病院消化器科
2）神戸朝日病院薬剤部
3）神戸朝日病院地域医療連携室
4）神戸大学大学院微生物学
5）兵庫県立がんセンター外科
6）順心病院外科
7）近畿大学消化器内科
8）神戸大学大学院遺伝病統御学分野
*Corresponding author: asahi-hp@arion.ocn.ne.jp
＜受付日2007年8月3日＞＜採択日2008年2月28日＞

Table 1 Host-dependent, virus related profile in the Elderly and Non-Elderly group

group	Elderly group	Non-Elderly group	*P*-value
Gender (M/F)	10/6	23/17	0.73
IFN treatment (retrial/naive)	4/9	22/17	0.11
HCV RNA level (KIU/mL)	2069±1380	1727±1581	0.35
HCV core antigen (fmol/L)	11058±13549	7256±7634	0.10
AST (IU/L)	40.4±19.4	46.3±33.7	0.96
ALT (IU/L)	39.8±19.9	52.9±38.0	0.39
Hb (g/dL)	13.7±1.39	13.9±1.65	0.93
WBC (/μL)	53.0±21.0	45.8±11.9	0.28
PLT (10^4/μL)	16.5±6.45	15.6±4.93	0.77
AFP (ng/mL)	10.1±9.55	12.0±29.9	0.30
HOMA-IR	11.5±17.5	5.70±5.63	0.20
BMI (%)	23.5±4.21	22.3±3.71	0.31
F0, 1/F2, 3	3/9	20/12	0.03

対象と方法

対象は，当院でPEG IFNα-2b/リバビリンの併用療法を48週行ない，2007年4月までに治療を終了した1b型高ウイルス量（HCV RNA定量ハイレンジ法で100 KIU/ml以上）C型慢性肝炎患者75名である．65歳以上の症例（以下，高齢群）23名（65歳～75歳　平均69.4歳　男性14名，女性9名），65歳未満の症例（以下，非高齢群）52名（28歳～64歳　平均53.5歳　男性33名，女性19名）である．両群間の患者背景をTable 1に記した．まず両群の著効率を検討した．著効とは，併用療法終了後6カ月においてもHCV-RNA陰性症例と定義した．又，全症例についてウイルスダイナミックスのマーカーとしてのHCVコア抗原減少率（測定時HCVコア抗原量/併用療法投与前　HCVコア抗原量）を24時間後，1週，2週，4週後に測定した．

HCVコア抗原量はIRMA法（fmol/L）（Ortho Clinical Diagnostics, Tokyo, Japan）で測定した．IFN誘導蛋白としての2-5AS（オリゴアデニレートシンゼターゼ）の応答率（測定時2-5AS量/併用療法投与前2-5AS量）を2，8，12，24，48週で測定した．2-5ASはRIA法（pmol/dL）（Eiken Immunochemical Laboratory, Tokyo, Japan）で測定した．治療前後のAFP値（ng/ml）を検討した．血球減少率はHb，白血球，血小板の減少率を4週から48週まで4週毎に測定した．治療を完遂した例について，PEG IFNα-2b及びリバビリンの減量症例数を検討した．治療を中断した症例について，両群とも中断症例数と中断した時期，中断の理由を検討した．

結　果

患者背景で高齢群で線維化が進行していたが（P＝0.03），それ以外の初回治療例の割合，男女比，HCV RNA量，HCVコア抗原量，AST値，ALT値，Hb値，白血球数，血小板数，AFP値，HOMA-IR，BMIでは両群間に差はなかった（Table 1）．著効率では，高齢群では37.5％（6/16），非高齢群では50％（20/40）で，統計学的に有意差はみられなかった（Fig. 1）．又，高齢群では男性の著効率は50％（3/6），女性は50％（3/6），性差はなく，非高齢群でも男性の著効率は65％（13/20）で女性は35％（7/20）で性差はなかった（P＝0.058）．

開始時と24時間後，1，2，4週後におけるコア抗原減少率においては，24時間後において高齢群でやや低い傾向はあったが（P＝0.069），1，2，4週間後では有意差はみられなかった（Fig 2）．2-5AS応答率のデーターでは，いずれの時点でも両群間に有意差は認めなかった（Fig 3）．

又，高齢群は著効例（AFP3.97±1.84 ng/ml）が非著効例（14.1±10.6 ng/ml）に比して開始時のAFP値が有意に低値であった（P＜0.01）（Fig. 4）．非高齢群では開始時のAFP値は著効例（5.27±4.08 ng/ml）と非著効例（18.7±41.6 ng/ml）との間に有意差はなかった（P＝0.125）．高齢群ではAFP値は治療前後で有意な低下がみられ（開始時10.1±9.55 ng/ml，終了時5.18±4.52 ng/ml）（P＜0.05），著効例（開始時3.97±1.84 ng/ml，

Fig. 1 The rate of sustained virologic response

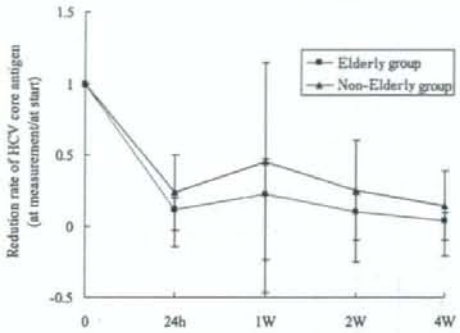

Fig. 2 The reduction rate of HCV core antigen

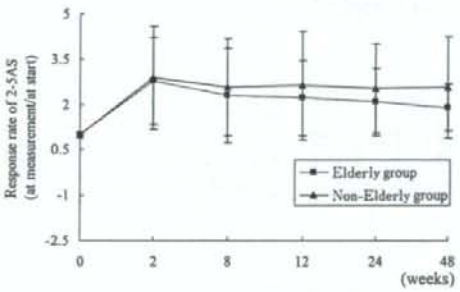

Fig. 3 The response rate of 2-5AS

終了時2.90±1.06 ng/ml) のみならず (P<0.05)，非著効例 (開始時14.1±10.6 ng/ml，終了時6.11±5.33 ng/ml) においてもみられた (P<0.05) (Fig. 4，Fig. 5)．非高齢群は開始時 AFP 値12.0±29.9 ng/ml であったが，終了時10.5±24.7 ng/ml で治療前後で有意差はなかった

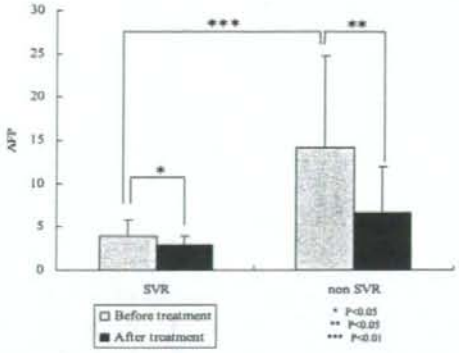

Fig. 4 The change of AFP values in the Elderly group

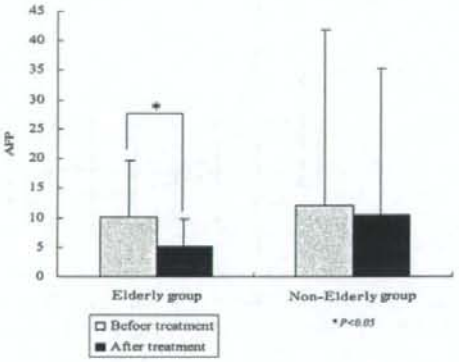

Fig. 5 The change of AFP values in the Elderly and Non-Elderly group

(P=0.052) (Fig. 5)．治療開始時から4週間毎のHb量の減少率では，20週で高齢群(高齢群減少率(0.72±0.077))は，非高齢群（非高齢群減少率 (0.78±0.093)) と比較して有意に低下していたが (P=0.033)，その他のいずれの時点でも両群間において差はなかった(Fig. 6)．白血球数の減少率では，いずれの時点でも両群間に有意差はみられなかった(Fig. 7)．血小板数の減少率についても，いずれの時点でも両群間で有意差はみられなかった (Fig. 8)．

治療を完遂した症例で，PEG IFNα-2b を減量した症例は全体で4例あり，高齢16例中1例 (6.2%)，非高齢群40例中3例 (7.5%) で両群間に差はなかった．

治療を完遂した症例で，リバビリンを減量した症例

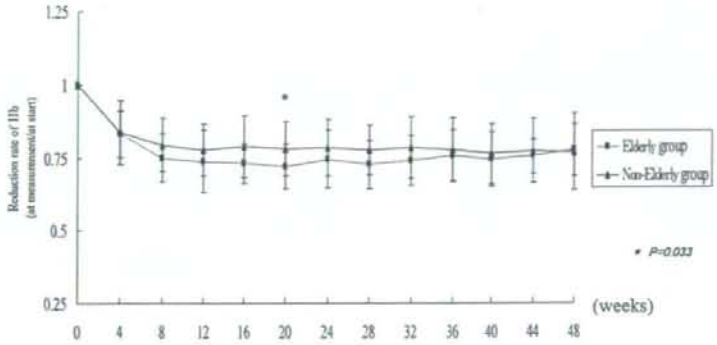

Fig. 6　The reduction rate of hemoglobin

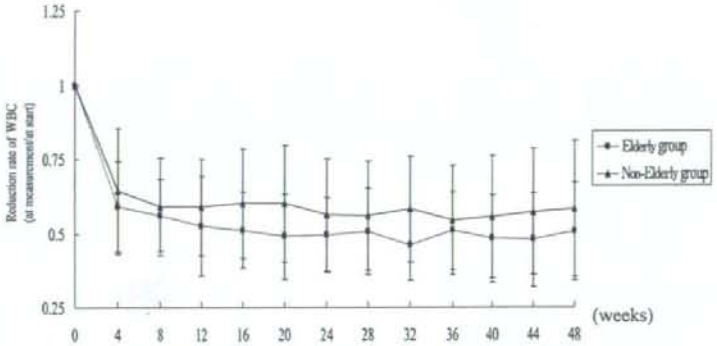

Fig. 7　The reduction rate of white blood cells

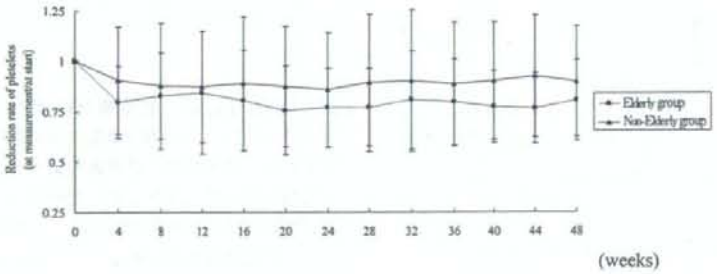

Fig. 8　The reduction rate of platelets

は全体で13例あり，高齢群16例中3例（18.8%），非高齢群40例中10例（25%）で両群間に差はなかった．治療を中断した19例について検討したところ，高齢群は23例中7例（30.4%），非高齢群は52例中12例（23.1%）で，両群間で中断率に差はみられなかった．治療を中断した理由として，高齢群は4週以内に4例57%（4/7）で，血小板数減少1例，発熱1例，全身倦怠2例，8週以内に全身倦怠1例で，20週以内に自己中断1例

Table 2　The cases of discontinuation

Elderly group		
4 weeks after therapy	4 cases	thrombocytopenia (1 case)
		high fever (1 case)
		general fatigue (2 cases)
8 weeks after therapy	1 case	general fatigue
20 weeks after therapy	1 case	self-discontinuation
45 weeks after therapy	1 case	interstitial pneumonia
Non-Elderly group		
4 weeks after therapy	5 cases	depression (1 case)
		self-discontinuation (2 cases)
		general fatigue (1 case)
		another disease (1 case)
8 weeks after therapy	3 cases	another disease (1 case)
		self-discontinuation (2 cases)
20 weeks after therapy	2 cases	self-discontinuation
24 weeks after therapy	2 cases	another disease (1 case)
		interstitial pneumonia (1 case)

で，45週に間質性肺炎1例であった．非高齢群は4週以内に5例41.7%(5/12)で，うつ症状が1例，自己中断が2例，全身倦怠が1例，他疾患治療が1例，8週以内に3例で，他疾患治療1例，自己中断2例，20週以内に自己中断が2例，24週以内に2例で，他疾患治療1例，間質性肺炎1例であった（Table 2）．

考　察

患者背景で線維化が高齢群に進行していた．初回治療例の割合，男女比，HCV RNA量，HCVコア抗原量，AST値，ALT値，Hb値，白血球数，血小板数，AFP値，HOMA-IR，BMIに両群間に差はなかった．併用療法のこれまでの治療成績をみると著効率に与える宿主因子として肝病理組織の脂肪化，線維化，閉経後の女性などの因子とともに高齢化が挙げられている[10]．しかし，我々の検討では著効率は高齢群と非高齢群との間に統計的には有意差はみられなかった．その原因として，今回の我々の検討では症例数が少なく，small groupによる検討であったことが関係している可能性がある．

又，高齢群と非高齢群との間に著効率に有意差がみられなかった要因としてウイルスダイナミックスのマーカー[14]としてのHCV抗原減少率[14~16]とIFN誘導蛋白の動態としての2-5AS応答率[15~17]とが両群間で同様な傾向を示し有意差を示さなかったことが挙げられる．C型慢性肝炎のIFN治療においてウイルスダイナミックスについてはIFNが直接肝細胞に働いて抗ウイルス蛋白を合成し，その作用により24時間以内でウイルスが急速に減少する投与後24時間までの第1期と，次いで上記の直接の抗ウイルス作用と細胞障害性Tリンパ球の働きによってC型肝炎ウイルス感染肝細胞が排除される投与後24時間から2週間までの第2期に分けられる[18~20,21]．1期，2期のいずれの時期においても高齢群と非高齢群においてウイルスダイナミックスすなわちHCV抗原減少率において差はみられなかった[19]．

2-5ASはIFNを投与された細胞で発見されたウイルスの増殖に必要な蛋白の阻害酵素であり，IFNの抗ウイルス活性と関係していることが確認された[22,23]．その後，2-5ASの上昇がIFN治療効果の予測に有用であることが示された[24~26]．ただ，今回の我々の検討では，2-5AS応答率はいずれの時点でも高齢群と非高齢群において差はみられなかった．

開始前のAFP値については高齢群と非高齢群の間に差はなかった．高齢群では治療前後でAFP値の低下がみられた．しかもそれは著効例のみならず，非著効例においてもみられた．非高齢群では治療前後にAFP値の有意の低下はみられていない．高齢群にみられた併用療法による治療前後のAFP値の低下がすべてIFNによる発癌抑制作用[27]によるものかどうかはにわかには断じがたい．AFP値低下が肝機能改善や線維化改善による可能性もあるからである．しかし，高齢群において併用療法の治療前後にみられたAFP値の低下は発癌抑制を何らかの形で反映していると考えてよいと思われる．それは60歳以上1b型高ウイルス量C型慢性肝炎患者の高齢者を対象としたIFN少量長期療法でAFP値が低下した症例からは発癌した症例がなかったという野村らの報告によっても支持される[28]．従って発癌抑制のためには高齢群において著効に至らなくても併用療法の完遂が重要である．又，高齢群における著効例は開始時のAFP値が非著効例に比較して有意に低値であった．芥田らは併用療法において開始前のAFP値が治療効果予測因子となること，その理由としてAFP値高値が線維化の進展を反映しているとしている[29]．今回我々の検討でも高齢群においては芥田らの報告と合致した．非高齢群では著効例と非著効例との間に開始時のAFP値に有意差はなかった．その理由は不明であるが，開始時AFP値が高齢群での治療効果予測因子の一つになることは重要な所見と考える．

我々の検討では患者背景として，高齢群はHb 13.7 g/dl，血小板16.5万/μl，白血球5300/μlであり，非高齢群はHb 13.9 g/dl，血小板15.6万/μl，白血球4580/μlで，高齢群と非高齢群では差はなかった．我々の今回の検討においては，併用療法後のHb，白血球，血小板などの血球の減少は20週目のHbが高齢群で有意に低下した以外，いずれの時点でも両群間に差はなかった．

治療を完遂した症例について，PEG IFNα-2bとリバビリンの減量率は両群間に差はなかった．このことも又，両群の著効率に差がなかった一つの要因として挙げられる．逆にいえば，高齢者のIFNとリバビリンの減量率を非高齢者と同様に抑えることができるなら，高齢群の著効率を非高齢群と同様に引き上げることができる．

中断症例についてみると，高齢群30.4％（7/23），非高齢群23.1％（12/52）と両群間に差はなかったが，その内容については差がみられた．すなわち高齢群においては4週目までは血小板数減少1例，発熱1例，全身倦怠2例で，8週目には全身倦怠1例，20週目に自己中断1例，45週目に間質性肺炎1例であった．非高齢群においては，4週以内5例で，その内容はうつ症状1例，自己中断2例，全身倦怠1例，他疾患治療1例であった．8週目までは3例で，他疾患治療1例，自己中断2例，20週目までは自己中断2例，24週目までは他疾患治療1例，間質性肺炎1例であった．特徴的なことは，65歳以上の高齢群で，開始後8週という早い時期に全身倦怠を訴えて中断した症例が中断症例5例中3例あったことである．非高齢群では，全身倦怠で中断した症例は中断症例10例中1例のみであった．高齢群の全身倦怠がリバビリンによる貧血によるものか，IFN投与による全身倦怠なのかは明らかでない．

1b型高ウイルス量高齢者C型慢性肝炎において併用療法が著効例のみならず，非著効例においても発癌抑制効果がみられたことは重要であり，治療の完遂こそが重要である．従って日常診療に従事する臨床医にあっては，高齢者の中断対策，とりわけ治療早期にみられる全身倦怠に対してきめ細かい対応が要求されている．そのことが1b型高ウイルス量高齢者C型慢性肝炎のIFN治療成績の向上及び発癌抑制につながるものと考えられる．

謝辞：本論文作成にあたり，御協力頂きました神戸朝日病院文書課・宮内　美奈子氏，川村　佳子氏，同薬剤部・笹瀬典子氏，神戸薬科大学病態生化学研究室・大山　紘一郎氏に感謝致します．

文　献

1) 戸川三省，山田剛太郎．高齢者C型慢性肝疾患へのインターフェロン治療．肝胆膵　2002；45：1033—1038
2) Hamada H, Yatsuhashi H, Yano K, et al. Impact of aging on the development of hepatocellular carcinoma in patients with posttransfusion chronic hepatitis C. Cancer 2002; 95 (2): 331—339
3) Yoshida H, Shiratori Y, Moriyama M, et al. Interferon therapy reduces the risk for hepatocellular carcinoma: National surveillance program of cirrhostic and noncirrhotic patients with chronic hepatitis C in Japan. Ann Intern Med 1999; 131: 174—181
4) Yoshizawa H. Trends of hepatitis virus carriers. Hepatol Res 2002; 24: S28—39

5) Nomura H, Tanimoto H, Kajiwara E, et al. Factors contributing to ribavirin-induced anemia. J Gastroen Hepatol 2004; 19: 1312—1317
6) Manns MP, McHutchison JG, Gordon SC, et al. Peginterferon alfa-2b plus ribavirin compared with interferon alfa-2b plus ribavirin for initial treatment of chronic hepatitis C: a randomised trial. Lancet 2001; 358: 958—965
7) Fried MW, Shiffman ML, Reddy KR, et al. Peginterferon alfa-2a plus ribavirin for chronic hepatitis C virus infection. N Engl J Med 2002; 347: 975—982
8) Romero-Gomez M, Del MV, Andrade RJ, et al. Insulin resistance impairs sustained response rate to peginterferon plus ribavirin in chronic hepatitis C patients. Gastroenterology 2005; 128 (3): 636—641
9) D'Souza R, Sabin CA, Foster GR. Insulin resistance plays a significant role in liver fibrosis in chronic hepatitis C and in the response to antiviral therapy. Am J Gastroenterol 2005; 100 (7): 1509—1515
10) Yaginuma R, Ikejima K, Okumura K, et al. Hepatic steatosis is a predictor of poor response to interferon alpha-2b and ribavirin combination therapy in Japanese patients with chronic hepatitis C. Hepatol Res 2006; 35: 19—25
11) Nomura H, Tanimoto H, Kajiwara E, et al. Factors contributing to ribavirin-induced anemia. J Gastroen Hepatol 2004; 19: 1312—1317
12) Hiramatsu N, Oze T, Tsuda N, et al. Should aged patients with chronic hepatitis C be treated with interferon and ribavirin combination therapy? Hepatol Res 2006; 35: 185—189
13) Okanoue T, Sakamoto S, Itoh Y, et al. Side effects of high-dose interferon therapy for chronic hepatitis C. J Hepatol 1996; 25: 283—291
14) Buti M, Mendez C, Schaper M, et al. Hepatitis C virus Core Antigen as a predictor of non-response in genotype 1 chronic hepatitis C patients treated with peginterferon α -2b plus ribavirin. J Hepatol 2004; 40: 527—532
15) Veillon P, Payan C, Pcchio G, et al. Comparative evaluation of the total hepatitis C virus core antigen, branched-DNA, and amplicor monitor assays in determining viremia for patients with chronic hepatitis C during interferon plus ribavirin combination therapy. J Clin Microbiol 2003; 41: 3212—3220
16) Zanetti AR, Romano L, Brunetto M, et al. Total HCV core antigen assay: a new marker of hepatitis C viremia for monitoring the progress of therapy. J Med Virol 2003; 70: 27—30
17) Kim KI, Kim SR, Sasase N, et al. 2'-, 5'-Oligoadenylate synthetase response ratio predicting virological response to PEG-interferon-α 2b plus ribavirin therapy in patients with chronic hepatitis C. J Clin Pharm Ther 2006; 31: 441—446
18) Yasui K, Okanoue T, Murakami Y, et al. Dynamics of hepatitis C viremia Following interferon-alpha administration. J Infect Dis 1998; 177: 1475—1479
19) Neumann AU, Lam NP, Dahari H, et al. Hepatitis C viral dynamics in vivo and the antiviral efficacy of interferon-alpha therapy. Science 1998; 282: 103—107
20) Anonymous. National Institutes of Health Consensus Development Conference Statement: Management of hepatitis C. Hepatology 2002; 36: S3
21) Anonymous. Consensus conference. Treatment of Hepatitis C. Agence Nationale d'Accreditation et d'Evaluation en Sante (ANAES). Gastroen Clin Biol 2002; 26: B303
22) Schmidt A, Zilberstein A, Shulman L, et al. Interferon action: isolation of nuclease F, a translation inhibitor activated by interferon-induced (2', 5') oligoisoadenylate. FEBS Lett 1978; 95: 257
23) Nilsen TW, McCandless S, Baglioni C. 2', 5'-oligo (A)-activated endonuclease in NIH 3T3 mouse cells chronically infected with Moloney murine leukemia virus. Virology 1982; 122: 498
24) Karino Y, Hige S, Matsushima M, et al. Significance of 2', 5'-oligoadenylate synthetase activity and HCV genotype in IFN therapy for type C chronic hepatitis. Hokkaido Igaku Zasshi 1994; 69: 1354
25) Toda K, Kumagai N, Iwabuchi N, et al. 2-5AS activity in serum and peripheral blood mononuclear cells for chronic active hepatitis C and the relationship to clinical outcome of interferon therapy. Jpn J Clin Immunol 1997; 20: 428
26) Tong WB, Zhang CY, Feng BF, et al. Establishment of a nonradioactive assay for 2', 5' oligoadenylate synthetase and its application in chronic hepatitis C patients receiving interferon-alpha. World J Gastroenterol 1998; 4: 70
27) Yano H, Yanai Y, Momosaki S, et al. Growth inhibi-

tory effects of interferon-α subtypes vary according to human liver cancer cell lines. J Gastroenterol Hepatol 2006; 21: 1720—1725
28) Nomura H, Kashiwagi Y, Hirano R, et al. Efficacy of low dose long-term interferon monotherapy in aged patients with chronic hepatitis C genotype 1 and its relation to alpha-fetoprotein: A Pilot study. Hepatol Res 2007; 37: 490—497
29) Akuta N, Suzuki F, Kawamura Y, et al. Predictors of viral kinetics to peginterferon plus rivavirin combination therapy in Japanese patients infected with hepatitis C virus genotype 1b. J Med Virol 2007; 79 (11): 1686—1695

Pegylated interferon α-2b/ribavirin combination therapy for elderly patients with chronic hepatitis C with high viral load of HCV genotype 1b

Soo Ryang Kim[1]*, Susumu Imoto[1], Shuichi Fuki[1], Ke Ih Kim[2], Miyuki Taniguchi[3], Motoko Nagano[4], Hak Hotta[4], Ikuo Shouji[4], Yoshihiro Kanbara[5], Yoko Maekawa[6], Masatoshi Kudo[7], Yoshitake Hayashi[8]

The patients (n = 75) in this study had chronic hepatitis C with high viral loads of serum HCV-RNA genotype 1b. All the patients received a regimen of pegylated interferon α-2b plus ribavirin (PEG IFN α-2b/RBV) for 48 weeks. Comparative analysis was done by dividing these patients into two groups by age: Elderly group (over 65 years old, 23 patients) and Non-Elderly group (under 65 years old, 52 patients). The sustained viral response (SVR) rate in the Elderly (37.5%, 6/16) was not different significantly from that in the Non-Elderly (50%, 20/40). The response ratio of 2′-5′-oligoadenylate synthetase (2-5AS), the viral dynamics and the rate of discontinuation of therapy were not different between the two groups. Interestingly, however, the mean α-fetoprotein (AFP) values decreased significantly in the Elderly irrespective of SVR or non-SVR (from 10.1 ± 9.55 ng/ml before treatment to 5.18 ± 4.52 ng/ml after treatment, $P<0.05$), but did not in the Non-Elderly. It was thus suggested that Peg IFN α-2b/RBV would be useful in the prevention of HCC in elderly patients including non-SVR cases.

Key words: chronic hepatitis C　pegylated interferon α-2b/ribavirin combination therapy　elderly patients　prevention of hepatocarcinogenesis　AFP

Kanzo 2008; 49: 145—152

1) Department of Gastroenterology, Kobe Asahi Hospital
2) Department of Pharmacy, Kobe Asahi Hospital
3) Medical Information Center, Kobe Asahi Hospital
4) Division of Microbiology, Kobe University Graduate School of Medicine
5) Department of Surgery, Hyogo Cancer Center
6) Department of Surgery, Junshin Hospital
7) Department of Gastroenterology, Kinki University Medical School of Medicine
8) Division of Molecular Medicine & Medical Genetics, Kobe University Graduate School of Medicine
*Corresponding author: asahi-hp@arion.ocn.ne.jp

ATF4-Mediated Induction of 4E-BP1 Contributes to Pancreatic β Cell Survival under Endoplasmic Reticulum Stress

Suguru Yamaguchi,[1,3] Hisamitsu Ishihara,[1,*] Takahiro Yamada,[1] Akira Tamura,[1] Masahiro Usui,[1] Ryu Tominaga,[1] Yuichiro Munakata,[1] Chihiro Satake,[1] Hideki Katagiri,[2] Fumi Tashiro,[4] Hiroyuki Aburatani,[5] Kyoko Tsukiyama-Kohara,[6] Jun-ichi Miyazaki,[4] Nahum Sonenberg,[7] and Yoshitomo Oka[1]

[1]Division of Molecular Metabolism and Diabetes
[2]Division of Advanced Therapeutics for Metabolic Diseases, Center for Translational and Advanced Animal Research
Tohoku University Graduate School of Medicine, Sendai, Miyagi 980-8575, Japan
[3]Institute for International Advanced Research and Education, Tohoku University, Sendai, Miyagi 980-8578, Japan
[4]Division of Stem Cell Regulation Research, Osaka University Graduate School of Medicine, Suita, Osaka 565-0871, Japan
[5]Research Center for Advanced Science and Technology, University of Tokyo, Tokyo 153-8904, Japan
[6]Department of Experimental Phylaxiology, Faculty of Medical and Pharmaceutical Sciences, Kumamoto University, Kumamoto 860-8556, Japan
[7]Department of Biochemistry and McGill Cancer Centre, McGill University, Montreal, QC H3G 1Y6, Canada
*Correspondence: hisamitsu-ishihara@mail.tains.tohoku.ac.jp
DOI 10.1016/j.cmet.2008.01.008

SUMMARY

Endoplasmic reticulum (ER) stress-mediated apoptosis may play a crucial role in loss of pancreatic β cell mass, contributing to the development of diabetes. Here we show that induction of 4E-BP1, the suppressor of the mRNA 5′ cap-binding protein eukaryotic initiation factor 4E (eIF4E), is involved in β cell survival under ER stress. 4E-BP1 expression was increased in islets under ER stress in several mouse models of diabetes. The *Eif4ebp1* gene encoding 4E-BP1 was revealed to be a direct target of the transcription factor ATF4. Deletion of the *Eif4ebp1* gene increased susceptibility to ER stress-mediated apoptosis in MIN6 β cells and mouse islets, which was accompanied by deregulated translational control. Furthermore, *Eif4ebp1* deletion accelerated β cell loss and exacerbated hyperglycemia in mouse models of diabetes. Thus, 4E-BP1 induction contributes to the maintenance of β cell homeostasis during ER stress and is a potential therapeutic target for diabetes.

INTRODUCTION

Recent studies have shown decreased pancreatic β cell mass to be a common feature of subjects with type 2 diabetes mellitus (Butler et al., 2003). Susceptibility to stress-induced apoptosis may underlie β cell loss. Translational regulation is an essential strategy by which cells cope with stress conditions (Clemens, 2001). Translation of eukaryotic mRNA is regulated primarily at the level of initiation. Translational initiation begins with formation of a ternary complex composed of the methionine-charged initiator tRNA, eukaryotic initiation factor 2 (eIF2), and GTP (Holcik and Sonenberg, 2005). The ternary complex then binds to the 40S ribosomal subunit and several other initiation factors, generating the 43S preinitiation complex. The mRNA 5′ cap-binding protein eIF4E associates with eIF4A and eIF4G to form the eIF4F complex and interacts with the 5′ cap structure of the mRNA. The eIF4F complex then recruits the 43S preinitiation complex to the mRNA, allowing the complex to scan toward the initiator AUG codon. The two best characterized regulatory steps in this translational control are formation of the ternary complex and assembly of the eIF4F complex. Phosphorylation of the α subunit of eIF2 (eIF2α) prevents ternary complex formation and thereby suppresses global translation. In addition, eIF4E-binding proteins (4E-BPs) inhibit eIF4F assembly by competitively displacing eIF4G from eIF4E. Global translational suppression through eIF2α phosphorylation is a mechanism shared among different stress-response pathways. Depending on the nature of the stress stimulus, eIF2α can be phosphorylated by four different kinases (Holcik and Sonenberg, 2005). Global attenuation of protein biosynthesis then paradoxically increases expression of several proteins, including the transcription factor ATF4 (Harding et al., 2000).

Because of their high insulin secretory activity, β cells are vulnerable to endoplasmic reticulum (ER) stress, a condition of disrupted ER homeostasis due to accumulation of misfolded proteins (Schroder and Kaufman, 2005). Cells respond to ER stress by activating an adaptive cellular response known as the unfolded protein response (UPR). Under ER stress conditions, global translation is suppressed through eIF2α phosphorylation by an ER-resident kinase, PERK. The importance of PERK-mediated translational suppression has been demonstrated in infancy-onset diabetes and skeletal defects caused by loss of PERK in humans (Delepine et al., 2000) and mice (Harding et al., 2001; Zhang et al., 2002). However, the roles of translational control through inhibition of eIF4F assembly by 4E-BPs under stress conditions, including ER stress, have yet to be fully clarified. Herein, we have studied roles of 4E-BP1,

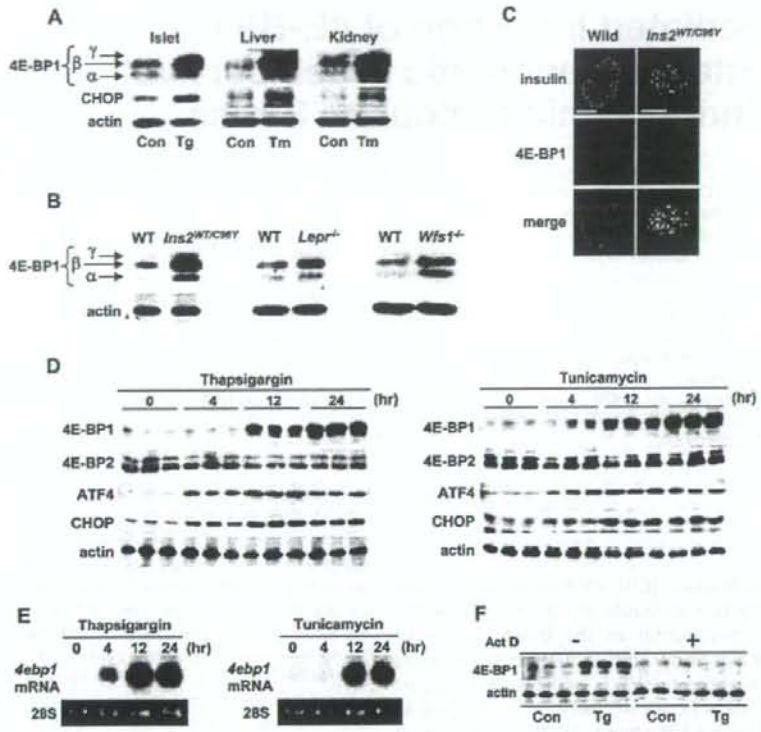

Figure 1. ER Stress Induces 4E-BP1 Expression

(A) Expression of 4E-BP1 protein in isolated islets treated with vehicle (0.05% DMSO) control (Con) or 0.5 μM thapsigargin (Tg) for 12 hr. 4E-BP1 expression was also examined in the livers and kidneys of mice that had received intraperitoneal injections of tunicamycin (Tm) 96 hr previously.

(B) Expression of 4E-BP1 protein in islets from wild-type (WT), *Ins2*$^{WT/C96Y}$, *Lepr*$^{-/-}$, and *Wfs1*$^{-/-}$ mice.

(C) Immunostaining of pancreatic sections from WT and *Ins2*$^{WT/C96Y}$ mice using anti-insulin and anti-4E-BP1 antibodies. Scale bars = 50 μm.

(D and E) Time courses of 4E-BP1, 4E-BP2, ATF4, and CHOP expression (D) and *4ebp1* mRNA expression (E) in MIN6 cells treated with thapsigargin (left panel) or tunicamycin (right).

(F) Inhibition of 4E-BP1 induction by actinomycin D (1 μg/ml) in MIN6 cells treated with thapsigargin for 12 hr.

one of three isoforms of the 4E-BP family, in β cells under ER stress.

RESULTS

ER Stress Induces 4E-BP1

4E-BP1 protein is present in three forms with different phosphorylation states. The hypophosphorylated α and β forms are active and the hyperphosphorylated γ form is inactive in terms of eIF4E binding. Expression of 4E-BP1 protein, especially the hypophosphorylated forms, was markedly induced, with an increase in CHOP, a stress marker protein, in isolated islets treated with thapsigargin (an ER Ca^{2+} pump inhibitor causing ER stress) (Figure 1A). 4E-BP1 induction was also observed in liver and kidneys of mice administered tunicamycin (a protein glycosylation inhibitor), another ER stress inducer (Figure 1A).

Furthermore, 4E-BP1 protein expression was markedly increased in *Ins2*$^{WT/C96Y}$ islets (Figures 1B and 1C), in which misfolded insulin molecules with a C96Y mutation cause ER stress (Wang et al., 1999). Islets from leptin receptor null (*Lepr*$^{-/-}$) mice, which have been shown to suffer from ER stress (Laybutt et al., 2007), also exhibited increased 4E-BP1 expression (Figure 1B). The *Wfs1*$^{-/-}$ mouse (Ishihara et al., 2004) is a model of Wolfram syndrome, which is characterized by juvenile-onset diabetes mellitus and optic atrophy and is caused by *WFS1* mutations (Inoue et al., 1998; Strom et al., 1998). WFS1-deficient islets are affected by chronic ER stress (Ishihara et al., 2004; Riggs et al., 2005). Again, 4E-BP1 protein was increased in *Wfs1*$^{-/-}$ islets (Figure 1B).

Induction of 4E-BP1 by ER stress was also observed in insulinoma MIN6 cells (Miyazaki et al., 1990) (Figure 1D). Expression of 4E-BP2, another member of the 4E-BP family, remained unchanged. While expression of ATF4 and CHOP peaked at 12 hr after treatment with thapsigargin or tunicamycin, 4E-BP1 protein was further increased at 24 hr posttreatment (Figure 1D). 4E-BP1 protein induction appeared to result from transcriptional

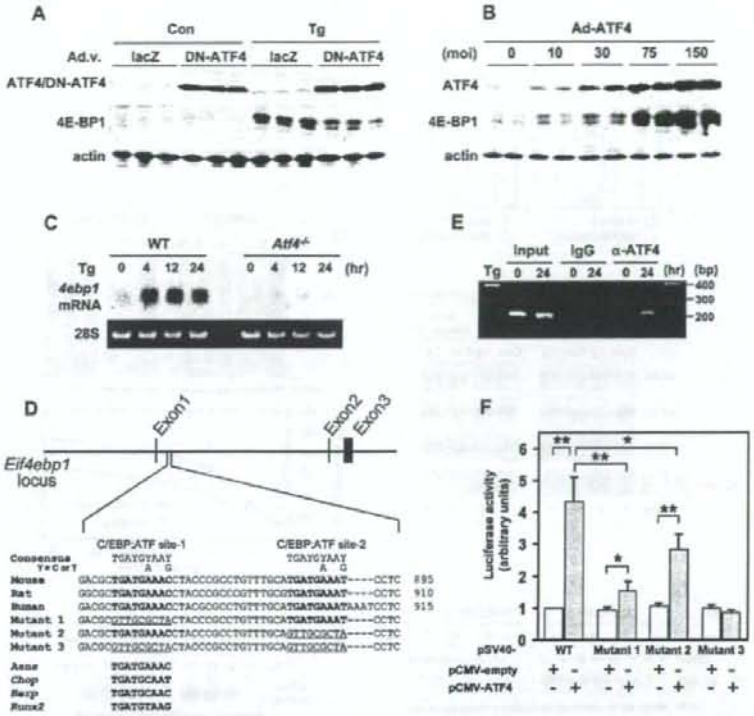

Figure 2. *Eif4ebp1* Is a Direct Target of ATF4

(A) Suppression of thapsigargin (Tg, 0.5 μM)-induced 4E-BP1 expression by dominant-negative ATF4 (DN-ATF4). MIN6 cells were infected with an adenovirus expressing either lacZ or DN-ATF4. Two days later, the cells were treated with vehicle (0.05% DMSO) control (Con) or Tg for 12 hr.

(B) 4E-BP1 expression in MIN6 cells infected with an adenovirus expressing wild-type ATF4 at the indicated multiplicity of infection (moi).

(C) *4ebp1* mRNA levels in wild-type and *Atf4*$^{-/-}$ MEFs treated with thapsigargin.

(D) C/EBP:ATF composite sites in intron 1 of the *Eif4ebp1* gene. Mouse, rat, and human *Eif4ebp1* gene segments are aligned with ATF4 binding sequences in several genes. Numbers are positions relative to A of the initial ATG codon. *Asns*, asparagine synthetase; *Herp*, homocysteine-induced ER protein; *Runx2*, runt-related transcription factor 2.

(E) Chromatin immunoprecipitation assay of MIN6 cells treated with thapsigargin. DNAs precipitated with nonspecific or anti-ATF4 IgG were amplified using primers for the *Eif4ebp1* intron 1 region.

(F) ATF4 induction of luciferase reporters with the *SV40* promoter and an *Eif4ebp1* gene segment with C/EBP:ATF composite sites or their mutants shown in (D). MIN6 cells were transfected with luciferase reporters together with either pCMV-empty or pCMV-ATF4. Error bars represent SEM. n = 4; *p < 0.05, **p < 0.01.

activation since *4ebp1* mRNA levels were also increased by these ER stress inducers (Figure 1E) and the transcriptional inhibitor actinomycin D completely blocked 4E-BP1 induction by thapsigargin (Figure 1F).

ATF4 Directly Activates the *Eif4ebp1* Gene

MIN6 cells were infected with recombinant adenoviruses expressing dominant-negative (DN) forms of transcription factors involved in the UPR. Expression of DN-ATF4 (He et al., 2001) (Figure 2A), but not DN-ATF6 or DN-XBP1 (see Figure S1 available online), suppressed 4E-BP1 induction by thapsigargin. Conversely, expression of wild-type ATF4 dramatically induced 4E-BP1 expression (Figure 2B). Furthermore, *4ebp1* mRNA levels were not increased by thapsigargin in *Atf4*$^{-/-}$ murine embryonic fibroblasts (MEFs) (Harding et al., 2003) (Figure 2C).

A survey of the mouse *Eif4ebp1* gene using a luciferase assay identified a segment in intron 1 that conferred thapsigargin sensitivity to a luciferase reporter (Figure S2). Indeed, we found two potential ATF4 binding sequences (C/EBP:ATF composite sites) in this segment (Figure 2D). Chromatin immunoprecipitation (ChIP) assays revealed that ATF4 binds this segment (Figure 2E). Furthermore, cotransfection of a luciferase reporter containing the C/EBP:ATF sites with an ATF4-expressing plasmid increased luciferase activity by 4.3-fold (Figure 2F). Disruption of the upstream C/EBP:ATF site (mutant 1) or the downstream site (mutant 2) decreased the ATF4-mediated increase in luciferase activity by 83% or 47%, respectively, and disruption of both (mutant 3) completely abolished the increase (Figure 2F).

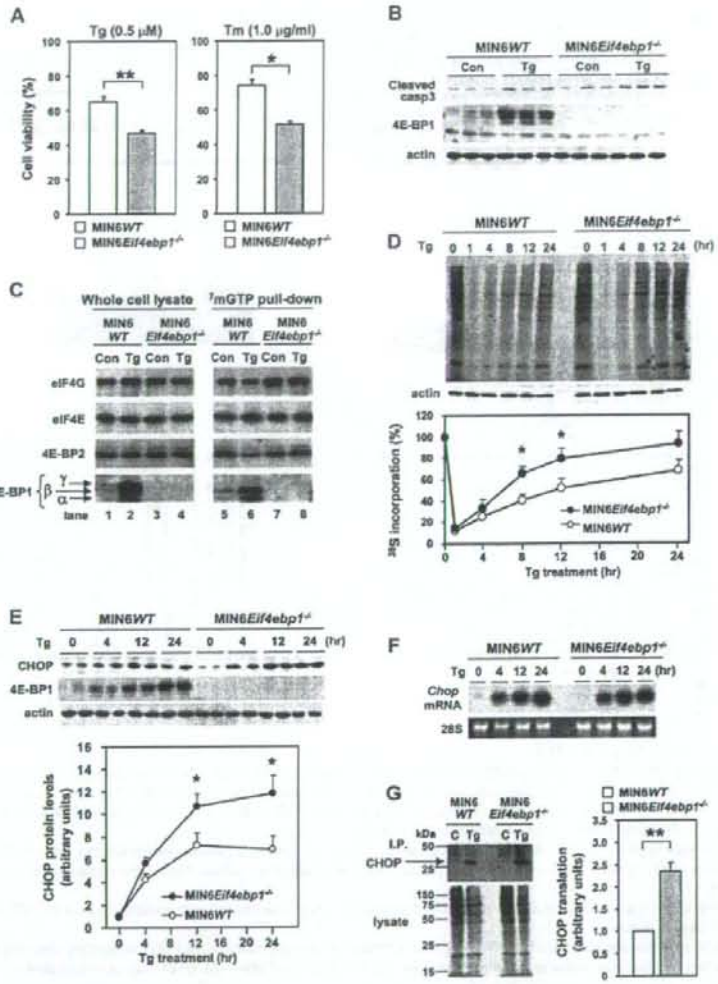

Figure 3. 4E-BP1-Deficient Cells Exhibit Increased Apoptosis Susceptibility with Deregulated Translational Control

(A) Viability of MIN6*WT* and MIN6*Eif4ebp1*$^{-/-}$ cells treated with 0.5 μM thapsigargin (Tg) or 1.0 μg/ml tunicamycin (Tm) for 36 hr, normalized to MIN6*WT* cells treated with vehicle (0.05% DMSO). n = 3–4.

(B) Immunoblot of cleaved caspase-3 in MIN6*WT* and MIN6*Eif4ebp1*$^{-/-}$ cells treated with vehicle control (Con) or thapsigargin for 24 hr.

(C) Immunoblot analysis of 4E-BP1, 4E-BP2, eIF4E, and eIF4G in whole-cell lysates (left) or in a complex associated with ^{7}mGTP-Sepharose (right) in cells treated with thapsigargin for 24 hr.

(D) [^{35}S]methionine/cysteine incorporation during a 15 min pulse labeling in MIN6*WT* and MIN6*Eif4ebp1*$^{-/-}$ cells pretreated with thapsigargin for the indicated periods. Ten percent of the lysates were also probed with an anti-actin antibody. A representative autoradiogram is shown in the upper panel; data from three experiments are summarized in the lower panel.

(E) Increased CHOP induction in MIN6*Eif4ebp1*$^{-/-}$ cells treated with thapsigargin. Representative blots are shown in the upper panel; data from four experiments are summarized in the lower panel.

(F) *Chop* mRNA levels in MIN6*WT* and MIN6*Eif4ebp1*$^{-/-}$ cells treated with thapsigargin.

(G) Greater *Chop* translation in MIN6*Eif4ebp1*$^{-/-}$ cells treated with thapsigargin. MIN6*WT* and MIN6*Eif4ebp1*$^{-/-}$ cells treated with vehicle (C) or thapsigargin (Tg) for 12 hr were labeled with [^{35}S]methionine/cysteine. Lysates were either directly subjected to SDS-PAGE or immunoprecipitated with anti-CHOP antibody. Representative autoradiograms are shown in the left panel; data from four experiments are summarized in the right panel.

Error bars represent SEM. *$p < 0.05$, **$p < 0.01$.

4E-BP1-Deficient β Cells Are More Vulnerable to ER Stress

A 4E-BP1-deficient β cell line, MIN6*Eif4ebp1*$^{-/-}$, was established by crossing *Eif4ebp1*$^{-/-}$ mice (Tsukiyama-Kohara et al., 2001) with IT6 mice expressing SV40 large T antigen in β cells (Miyazaki et al., 1990). MIN6 cells with wild-type *Eif4ebp1* alleles, established in parallel, were designated MIN6*WT* cells. MIN6*Eif4ebp1*$^{-/-}$ cells were more vulnerable to ER stress inducers than MIN6*WT* cells (Figure 3A). 4E-BP1 re-expression restored this diminished viability of MIN6*Eif4ebp1*$^{-/-}$ cells to control levels (Figure S3A). The increased susceptibility to ER stress-induced cell death was accompanied by enhanced caspase-3 cleavage (Figure 3B), indicating that the reduced viability of MIN6*Eif4ebp1*$^{-/-}$ cells was due at least in part to increased apoptosis. In addition, DNA fragmentation under ER stress was greater in *Eif4ebp1*$^{-/-}$ islets than in wild-type islets (Figure S3B). These results suggest that 4E-BP1 induction contributes to β cell survival under ER stress.

We then examined the impact of 4E-BP1 deficiency on the integrity of the eIF4F translational initiation complex. Pull-down assays of eIF4E and its binding partners with a cap analog, 7-methyl-GTP, revealed that thapsigargin-induced 4E-BP1 expression resulted in marked increases in the amounts of hypophosphorylated 4E-BP1 α and β forms bound to eIF4E, displacing eIF4G from eIF4E in MIN6*WT* cells (Figure 3C, compare lane 5 with lane 6). The amount of eIF4G bound to eIF4E was reduced to 63% ± 3% ($n = 4$, $p < 0.05$) of that in vehicle-treated MIN6WT cells. In contrast, levels of eIF4G bound to eIF4E were not decreased by thapsigargin in MIN6*Eif4ebp1*$^{-/-}$ cells (Figure 3C, compare lane 7 with lane 8). Thus, eIF4E availability for translational initiation was greater in MIN6*Eif4ebp1*$^{-/-}$ cells than in MIN6*WT* cells under ER stress. Measurement of the global translation rate revealed that recovery from translational suppression by thapsigargin was more rapid in 4E-BP1-deficient cells (Figure 3D).

Translation of newly synthesized mRNA molecules is reportedly much more dependent on eIF4E availability than that of preexisting mRNAs (Novoa and Carrasco, 1999). Expression of CHOP, a mediator of ER stress-induced apoptosis, was thus studied in MIN6*Eif4ebp1*$^{-/-}$ cells since *Chop* mRNA is one of the transcripts most abundantly synthesized during ER stress (Pirot et al., 2007). *Eif4ebp1* deletion caused greater CHOP protein induction by thapsigargin in MIN6 cells (Figure 3E), with unaltered *Chop* mRNA accumulation (Figure 3F). Pulse-labeling experiments demonstrated enhanced CHOP translation (Figure 3G). Thus, CHOP expression during ER stress was augmented via increased translation in 4E-BP1 deficiency.

Eif4ebp1 Deletion Accelerates β Cell Loss in Mouse Diabetes Models

To examine the roles of 4E-BP1 under ER stress in vivo, *Eif4ebp1*$^{-/-}$ mice on the 129S6 background were fed a high-fat diet (HFD), which is thought to produce ER stress in β cells through peripheral insulin resistance (Scheuner et al., 2005). *Eif4ebp1*$^{-/-}$ mice developed glucose intolerance (Figures S4A and S4B), which was associated with blunted insulin secretion (Figure S4C) and reduced pancreatic insulin content (Figure S4D) as compared to HFD-fed wild-type mice. These data suggest that *Eif4ebp1*$^{-/-}$ mice have a β cell defect. However, HFD-fed *Eif4ebp1*$^{-/-}$ mice gained more weight and were more insulin resistant than HFD-fed wild-type mice (Figures S4E and S4F). Therefore, the possibility remains that β cell failure in HFD-fed *Eif4ebp1*$^{-/-}$ mice resulted from greater ER stress rather than from a defect in β cells lacking 4E-BP1.

We next crossed *Eif4ebp1*$^{-/-}$ mice with two genetic models of diabetes in which β cells are under ER stress, *Ins2*$^{WT/C96Y}$ and *Wfs1*$^{-/-}$ mice on the 129S6 background. 4E-BP1 deficiency did not alter body weight (Figures S5A and S5B) or insulin sensitivity (Figures S5C and S5D) but worsened hyperglycemia in *Ins2*$^{WT/C96Y}$ (Figure 4A) and *Wfs1*$^{-/-}$ (Figure 4B) mice. In *Eif4ebp1*$^{-/-}$ *Ins2*$^{WT/C96Y}$ mice, pancreatic insulin content was less than half of that in *Ins2*$^{WT/C96Y}$ mice at 5 weeks of age (Figure 4C), and the majority of islets in *Eif4ebp1*$^{-/-}$ *Ins2*$^{WT/C96Y}$ mice were smaller as compared to those in *Ins2*$^{WT/C96Y}$ mice (Figure 4D). We also observed a 38% decrease in pancreatic insulin content in *Eif4ebp1*$^{-/-}$ *Wfs1*$^{-/-}$ mice as compared to *Wfs1*$^{-/-}$ mice (Figure 4E). Importantly, the insulin-positive area was smaller in pancreatic sections from *Eif4ebp1*$^{-/-}$ *Wfs1*$^{-/-}$ mice than in pancreatic sections from *Wfs1*$^{-/-}$ mice at 27–30 weeks of age (Figure 4F), indicating that ER stress-mediated β cell loss is exacerbated by 4E-BP1 deficiency in vivo.

Global protein synthesis was studied in these mouse islets. A tendency toward decreased protein synthesis was observed in both *Ins2*$^{WT/C96Y}$ (Figure 4G, hatched bar; $p = 0.074$) and *Wfs1*$^{-/-}$ islets (Figure 4H, hatched bar; $p = 0.079$) as compared to wild-type islets. *Eif4ebp1* deletion ablated this regulation and resulted in significantly increased protein synthesis in *Eif4ebp1*$^{-/-}$ *Ins2*$^{WT/C96Y}$ ($p = 0.013$) and *Eif4ebp1*$^{-/-}$ *Wfs1*$^{-/-}$ ($p = 0.045$) islets as compared to that in corresponding single mutants (compared hatched with filled bars in Figures 4G and 4H). These data suggest that accelerated β cell loss under ER stress is due to deregulated translational control.

DISCUSSION

Our results implicate 4E-BP1, identified as a component of the UPR, in β cell survival under ER stress. Important roles of 4E-BPs under various stress conditions have been recently demonstrated in yeast (Ibrahimo et al., 2006) and *Drosophila* (Teleman et al., 2005; Tettweiler et al., 2005). These data suggest that translational suppression by 4E-BPs is an evolutionarily conserved strategy against stress conditions. Although we focused on β cells, ER stress-mediated induction of 4E-BP1 was also observed in the liver and kidneys, suggesting the general importance of the present findings.

Our results suggest that, in addition to translational regulation by eIF2α phosphorylation due to PERK activation, another mode of translational control mediated by 4E-BP1 plays a role in the maintenance of β cell homeostasis under ER stress. Since translational suppression by eIF2α phosphorylation is transient owing to feedback dephosphorylation by GADD34 (Novoa et al., 2001), prolonged translational suppression by 4E-BP1 might be needed in the later stages of the UPR. However, in contrast to PERK, 4E-BP1 deficiency alone does not cause diabetes in mice under normal conditions, suggesting that 4E-BP1 protein is not a key regulator but rather functions with other molecules to maintain β cell homeostasis under ER stress. The preferential role of 4E-BP1 in the later stages of the UPR might be puzzling since expression of